

Motion of the Tippe Top

Gyroscopic Balance Condition and Stability

TAKAHIRO UEDA*, KEN SASAKI† AND SHINSUKE WATANABE‡

*Dept. of Physics, Faculty of Engineering, Yokohama National University
Yokohama 240-8501, JAPAN*

Abstract

We reexamine a very classical problem, the spinning behavior of the tippe top on a horizontal table. The analysis is made for an eccentric sphere version of the tippe top, assuming a modified Coulomb law for the sliding friction, which is a continuous function of the slip velocity \mathbf{v}_P at the point of contact and vanishes at $\mathbf{v}_P = \mathbf{0}$. We study the relevance of the gyroscopic balance condition (GBC), which was discovered to hold for a rapidly spinning hard-boiled egg by Moffatt and Shimomura, to the inversion phenomenon of the tippe top. We introduce a variable ξ so that $\xi = 0$ corresponds to the GBC and analyze the behavior of ξ . Contrary to the case of the spinning egg, the GBC for the tippe top is not fulfilled initially. But we find from simulation that for those tippe tops which will turn over, the GBC will soon be satisfied approximately. It is shown that the GBC and the geometry lead to the classification of tippe tops into three groups: The tippe tops of Group I never flip over however large a spin they are given. Those of Group II show a complete inversion and the tippe tops of Group III tend to turn over up to a certain inclination angle θ_f such that $\theta_f < \pi$, when they are spun sufficiently rapidly. There exist three steady states for the spinning motion of the tippe top. Giving a new criterion for stability, we examine the stability of these states in terms of the initial spin velocity n_0 . And we obtain a critical value n_c of the initial spin which is required for the tippe top of Group II to flip over up to the completely inverted position.

*e-mail address: t-ueda@phys.ynu.ac.jp

†e-mail address: sasaki@phys.ynu.ac.jp

‡e-mail address: wtnb@ynu.ac.jp

1 Introduction

Spinning objects have historically been interesting subjects to study. The spin reversal of the rattleback [1] (also called a celt or wobblestone) and the behavior of the tippe top are typical examples. In the latter case, when a truncated sphere with a cylindrical stem, a so-called ‘tippe top’, is spun sufficiently rapidly on a table with its stem up, it will flip over and rotate on its stem. This inversion phenomenon has fascinated physicists and has been studied for over a century [2, 3, 4, 5, 6, 7, 8, 9].

In the present paper we revisit and study this very classical problem from a different perspective. Recently the riddle of spinning eggs has been resolved by Moffatt and Shimomura [MS] [10]. They discovered that if an axisymmetric body, such as a hard-boiled egg, is spun sufficiently rapidly, a ‘*gyroscopic balance*’ condition (GBC) holds and that under this condition the governing equations of the system are much simplified. In particular, they derived a first-order ordinary differential equation (ODE) for θ , the angle between the axis of symmetry and the vertical axis, and showed for the case of a prolate spheroid that the axis of symmetry indeed rises from the horizontal to the vertical. Then the spinning behavior of egg-shaped axisymmetric bodies, whose cross sections are described by several models of oval curves, was studied under the GBC by one of the present authors [11].

The tippe top is also an axisymmetric body and shows the similar behavior as the spinning egg. Then one may ask: does the GBC also hold for the tippe top? If so, how is it related to the inversion phenomenon of the tippe top? In the first half of this paper we analyze the spinning motion of the tippe top in terms of the GBC. Actually the GBC is not satisfied initially for the tippe top, contrary to the case of the spinning egg. The difference comes from how we start to spin the object: we spin the tippe top with its stem up, in other words, with its symmetry axis vertical while the egg is spun with its symmetry axis horizontal. In this paper we perform our analysis taking an eccentric sphere version of the tippe top instead of a commercially available one, a truncated sphere with a cylindrical stem. In order to examine the GBC of the tippe top more closely, we introduce a variable ξ so that $\xi = 0$ corresponds to the GBC, and study the behavior of ξ . Numerical analysis shows that for the tippe tops which will turn over, the variable ξ , starting from a

large positive value ξ_0 , soon takes negative values and fluctuates around a negative but small value ξ_m such that $|\xi_m/\xi_0| \approx 0$. Thus for these tippe tops, the GBC, which is not satisfied initially, will soon be realized but approximately. On the other hand, in the case of the tippe tops which will not turn over, ξ remains positive around ξ_0 or changes from positive ξ_0 to negative values and then back to positive values close to ξ_0 again. We find that the behavior of ξ is closely related to the inversion phenomenon of the tippe top. Once ξ fluctuates around the value ξ_m , the system becomes unstable and starts to turn over.

Under the GBC the governing equations for the tippe top are much simplified and we obtain a first-order ODE for θ , which has the same form as the one derived by MS for the spinning egg. Then, this equation for θ and the geometry lead to the classification of tippe tops into *three* groups, depending on the values of $\frac{A}{C}$ and $\frac{a}{R}$, where A and C are two principal moments of inertia, and a is the distance from the center of sphere to the center of mass and R is the radius of sphere. The tippe tops of Group I never flip over however large a spin they are given. Those of Group II show a complete inversion and the tippe tops of Group III tend to turn over up to a certain inclination angle θ_f such that $\theta_f < \pi$, when they are spun sufficiently rapidly. This classification of tippe tops into three groups and its classificatory criteria totally coincide with those obtained by Hugenholtz [3] and Leutwyler [6], both of whom resorted to completely different arguments and methods.

In the latter half of this paper we study the steady states for spinning motion of the tippe top and examine their stability (or instability). It is well understood that the main source for the tippe top inversion is sliding friction [2, 3], which depends on the slip velocity \mathbf{v}_P of the contact point between the tippe top and a table. Often used is Coulomb friction (see Eq.(2.13)). In fact, Coulomb friction is practical when $|\mathbf{v}_P|$ is away from zero, but it is undefined for $\mathbf{v}_P = 0$. However, we learn that at the steady state of the tippe top, the slip velocity \mathbf{v}_P necessarily vanishes. In order to facilitate a linear stability analysis of steady states and also to study the motion of the tippe top as realistically as possible, we adopt in our analysis a modified version of Coulomb friction (see Eq.(2.14)), which is continuous in \mathbf{v}_P and vanishes at $\mathbf{v}_P = \mathbf{0}$.

Actually the steady states of the tippe top and their stability were analyzed by Ebenfeld and Scheck [ES] [7], who assumed a similar frictional force which is continuous at $\mathbf{v}_P = \mathbf{0}$. They used the total energy of the spinning top as a Liapunov function. The steady states were found as solutions of constant energy. And the stability or instability of these states were judged by examining whether the Liapunov function assumes a minimum or a maximum at these states. Also recently, Bou-Rabee, Marsden and Romero [BMR] [9] analyzed the tippe top inversion as a dissipation-induced instability and, using the modified Maxwell-Bloch equations and an energy-momentum argument, they gave criteria for the stability of the non-inverted and inverted states of the tippe top.

We take a different approach to this problem. First, in order to find the steady states for spinning motion of the tippe top, we follow the method used by Moffatt, Shimomura and Branicki [MSB] for the case of spinning spheroids [12]. Then the stability of these steady states is examined as follows: Once a steady state is known, the system is perturbed around the steady state. Particularly we focus our attention on the variable θ , which is perturbed to $\theta = \theta_s + \delta\theta$, where θ_s is a value at the steady state and $\delta\theta$ is a small quantity. Using the equations of motion, we obtain, under the linear approximation, a first-order ODE for $\delta\theta$ of the form, $\delta\dot{\theta} = H_s\delta\theta$, where H_s is expressed by the values of dynamical variables at the steady state. Thus the change of $\delta\theta$ is governed by the sign of H_s . If H_s is positive (negative), $|\delta\theta|$ will increase (decrease) with time. Therefore, we conclude that when H_s is negative (positive), then the state is stable (unstable). Using this new and rather intuitive criterion we argue about the stability of the steady states in terms of the initial spin velocity n_0 given at the position near $\theta=0$. We observe that our results on the stability of the steady states are consistent with ones obtained by ES and MSB. Then we obtain a critical value n_c of the initial spin which is required for the tippe top of Group II to flip over up to the completely inverted position at $\theta = \pi$. Finally we confirm by simulation our results on the relation between the initial spin n_0 and the stability of the steady states.

The paper is organized as follows: In Sec. 2 we explain the notation and geometry used in this paper, and give all the necessary equations for the analysis of the

spinning motion of the tippe top. In Sec. 3 we discuss about the GBC and its relevance to the inversion phenomenon of the tippe top. We also show that the assumption of the GBC leads to the classification of tippe tops into three groups. Then in Sec. 4 we study the steady states for the spinning motion of the tippe top and examine their stability. Sec. 5 is devoted to a summary and discussion. In addition, we present four appendices. In Appendix A, the equations of motion which are used to analyze the spinning motion of the tippe top are enumerated. In Appendix B, it is shown that intermediate steady states for the tippe tops of Group II and Group III are stable when an initial spin $n(\theta = 0)$ falls in a certain range. In Appendix C we demonstrate that our stability criterion for the steady state is equivalent to the one obtained by ES. And finally, in Appendix D, we show that our results on the stability of the vertical spin states are consistent with the criteria derived by BMR.

2 Equations of motion for tippe tops

A commercially available tippe top is usually a truncated sphere with a cylindrical stem. Instead we perform our analysis taking a loaded (eccentric) sphere version of the tippe top. The center of mass is off center by a distance a . There are no qualitative differences between the two. But if applied to the case of a commercial tippe top with a stem, our assertions would be valid up to the point when the stem touched the table surface.

Fig. 1 shows the geometry. An axisymmetric tippe top spins on a horizontal table with point of contact P . We will work in a rotating frame of reference $OXYZ$, where the center of mass is at the origin, O . The center S of the sphere with radius R is at a distance a from the origin. The symmetry axis of the tippe top, Oz , and the vertical axis, OZ , define a plane Π , which precesses about OZ with angular velocity $\boldsymbol{\Omega}(t) = (0, 0, \Omega)$. Let (ϕ, θ, ψ) be the Euler angles of the body relative to OZ . Then we have $\Omega = \dot{\phi}$, where the dot represents differentiation with respect to time, and θ is the angle between OZ and Oz . We choose the horizontal axis OX in the plane Π

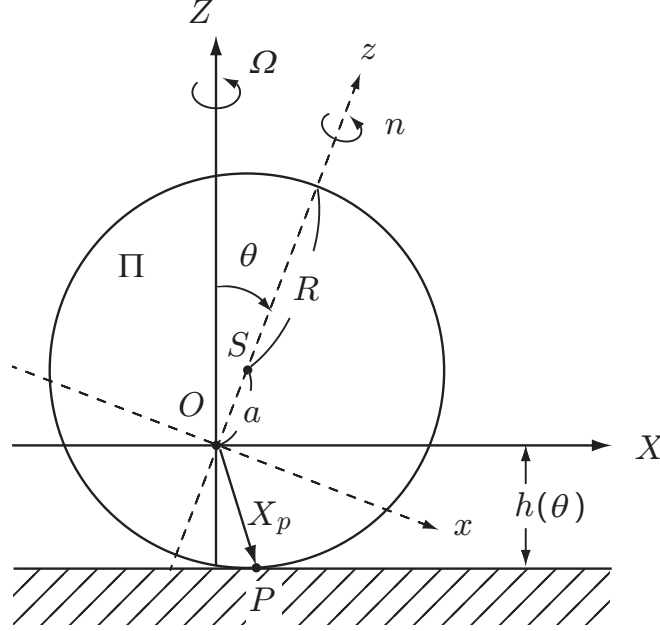


Figure 1: A loaded sphere (eccentric) version of the tippe top. The center of mass O is off center (S) by distance a . The tippe top spins on a horizontal table with point of contact P . Its axis of symmetry, Oz , and the vertical axis, OZ , define a plane Π , which precesses about OZ with angular velocity $\boldsymbol{\Omega}(t) = (0, 0, \Omega)$. $OXYZ$ is a rotating frame of reference with OX horizontal in the plane Π . The height of O above the table is $h(\theta) = R - a \cos \theta$, where R is the radius. The position vector of P from O is $\mathbf{X}_P = (X_P, 0, Z_P)$, where $X_P = \frac{dh}{d\theta}$ and $Z_P = -h(\theta)$.

and thus OY is vertical to Π and inward.

In a rotating frame of reference $Oxyz$, where Ox is in the plane Π and perpendicular to the symmetry axis Oz and where Oy coincides with OY , the tippe top spins about Oz with the rate $\dot{\psi}$. Since $\boldsymbol{\Omega}$ is expressed as $\boldsymbol{\Omega} = -\Omega \sin \theta \hat{\mathbf{x}} + \Omega \cos \theta \hat{\mathbf{z}}$ in the frame $Oxyz$, the angular velocity of the tippe top, $\boldsymbol{\omega}$, is given by $\boldsymbol{\omega} = -\Omega \sin \theta \hat{\mathbf{x}} + \dot{\theta} \hat{\mathbf{y}} + n \hat{\mathbf{z}}$. Here $\hat{\mathbf{x}}$, $\hat{\mathbf{y}}$, and $\hat{\mathbf{z}}$ are unit vectors along Ox , Oy , and Oz , respectively, $n(t)$ is given by $n = \Omega \cos \theta + \dot{\psi}$. The Ox and Oy are not body-fixed axes but are principal axes, so that the angular momentum, \mathbf{L} , is expressed by $\mathbf{L} = -A\Omega \sin \theta \hat{\mathbf{x}} + A\dot{\theta} \hat{\mathbf{y}} + Cn \hat{\mathbf{z}}$, where (A, A, C) are the principal moments of inertia at O . Using the perpendicular axis theorem and the parallel axis theorem, we see

that $A/C \geq \frac{1}{2}$ for any axisymmetric density distribution.

The coordinate system $Oxyz$ is obtained from the frame $OXYZ$ by rotating the latter about the OY (Oy) axis through the angle θ . Hence, in the rotating frame $OXYZ$, $\boldsymbol{\omega}$ and \mathbf{L} have components

$$\boldsymbol{\omega} = \left((n - \Omega \cos \theta) \sin \theta, \dot{\theta}, \Omega \sin^2 \theta + n \cos \theta \right), \quad (2.1)$$

$$\mathbf{L} = \left((Cn - A\Omega \cos \theta) \sin \theta, A\dot{\theta}, A\Omega \sin^2 \theta + Cn \cos \theta \right), \quad (2.2)$$

respectively. The evolution of \mathbf{L} is governed by Euler's equation

$$\frac{\partial \mathbf{L}}{\partial t} + \boldsymbol{\Omega} \times \mathbf{L} = \mathbf{X}_P \times (\mathbf{N} + \mathbf{F}), \quad (2.3)$$

where \mathbf{X}_P is the position vector of the contact point P from O , \mathbf{N} is the normal reaction at P , $\mathbf{N} = (0, 0, N)$, with N being of order Mg , the weight, and $\mathbf{F} = (F_X, F_Y, 0)$ is the frictional force at P . We consider only *the situation in which the tippe top is always in contact with the table* throughout the motion. Since the point P lies in the plane Π , \mathbf{X}_P has components $(X_P, 0, Z_P)$, which are given by

$$Z_P = -(R - a \cos \theta) \equiv -h(\theta), \quad (2.4a)$$

$$X_P = a \sin \theta = \frac{dh}{d\theta}, \quad (2.4b)$$

where $h(\theta)$ is the height of O above the table. The components of (2.3) are expressed, respectively, as

$$\dot{L}_X - \Omega L_Y = h(\theta) F_Y, \quad (2.5a)$$

$$\dot{L}_Y + \Omega L_X = -a \sin \theta N - h(\theta) F_X, \quad (2.5b)$$

$$\dot{L}_Z = a \sin \theta F_Y. \quad (2.5c)$$

In terms of θ , Ω , and n the above equations are rewritten as

$$A\dot{\Omega} \sin \theta = (Cn - 2A\Omega \cos \theta)\dot{\theta} + (a - R \cos \theta)F_Y, \quad (2.6a)$$

$$A\ddot{\theta} = -\Omega(Cn - A\Omega \cos \theta) \sin \theta - a \sin \theta N - h(\theta)F_X, \quad (2.6b)$$

$$C\dot{n} = R \sin \theta F_Y. \quad (2.6c)$$

Now it is easily seen from (2.2), (2.5a) and (2.5c) that there exists an exact constant of motion,

$$J = -\mathbf{L} \cdot \mathbf{X}_P = -L_X \frac{dh}{d\theta} + L_Z h(\theta) \quad (\text{a constant}), \quad (2.7)$$

which is valid irrespective of the reaction force $(\mathbf{N} + \mathbf{F})$ at the contact point P , in other words, whether or not slipping occurs. This so-called “Jellett’s constant” [13] is typical for the tippe top whose portion of the surface in contact with the table is spherical.

The velocity, $\mathbf{v}_{\text{rot}P}$, of the contact point P with respect to the center of mass O is given by $\mathbf{v}_{\text{rot}P} = \boldsymbol{\omega} \times \mathbf{X}_P$, and thus has components,

$$v_{\text{rot}PX} = -h(\theta)\dot{\theta}, \quad (2.8a)$$

$$v_{\text{rot}PY} = \{R(n - \Omega \cos \theta) + a\Omega\} \sin \theta, \quad (2.8b)$$

$$v_{\text{rot}PZ} = -a \sin \theta \dot{\theta}. \quad (2.8c)$$

The center of mass O is not stationary. Let $\mathbf{u}_O = (u_{OX}, u_{OY}, u_{OZ})$ represent the velocity of O , then the slip velocity of the contact point P , $\mathbf{v}_P = (v_{PX}, v_{PY}, v_{PZ})$, is

$$\mathbf{v}_P = \mathbf{u}_O + \mathbf{v}_{\text{rot}P}. \quad (2.9)$$

Since $u_{OZ} = \frac{dh}{dt} = -v_{\text{rot}PZ}$, we have $v_{PZ} = 0$ as was expected.

The equation of motion for the center of mass O is given by

$$M \left(\frac{\partial \mathbf{u}_O}{\partial t} + \boldsymbol{\Omega} \times \mathbf{u}_O \right) = \mathbf{N} + \mathbf{F} + \mathbf{W}, \quad (2.10)$$

where M is the mass of the tippe top and $\mathbf{W} = (0, 0, -Mg)$ is the force of gravity. In components, Eq.(2.10) reads

$$M (\dot{u}_{OX} - \Omega u_{OY}) = F_X, \quad (2.11a)$$

$$M (\dot{u}_{OY} + \Omega u_{OX}) = F_Y, \quad (2.11b)$$

$$M \dot{u}_{OZ} = N - Mg. \quad (2.11c)$$

Since $\dot{u}_{OZ} = \frac{d^2 h}{dt^2}$, Eq.(2.11c) gives

$$N = M \left\{ g + a \left(\dot{\theta}^2 \cos \theta + \ddot{\theta} \sin \theta \right) \right\}, \quad (2.12)$$

which shows that the normal force N is of order Mg when $a\dot{\theta}^2$, $a|\ddot{\theta}| \ll g$.

We need an information on the frictional force \mathbf{F} . It is well understood that the sliding friction is the main source for the tippe top inversion [2, 3]. So we will ignore other possible frictions, such as, rolling friction [14] and rotational friction which is due to pure rotation about a vertical axis .

Concerning the sliding friction, often used is a Coulomb law, which states that

$$\mathbf{F}_C = -\mu N \frac{\mathbf{v}_P}{|\mathbf{v}_P|} . \quad (2.13)$$

where μ is a coefficient of friction. Another possibility is a viscous friction law, which states that the friction is linearly related to \mathbf{v}_P . Coulomb friction is practical when $|\mathbf{v}_P|$ is away from zero but it is undefined at $\mathbf{v}_P = 0$. The slip velocity of the contact point P necessarily vanishes at the steady state of the tippe top. In order to study the motion of the tippe top as realistically as possible and also to facilitate a linear stability analysis of steady states, we modify the expression of Coulomb friction (2.13) as

$$\mathbf{F} = -\mu N \frac{\mathbf{v}_P}{|\mathbf{v}_P(\Lambda)|} , \quad \text{with} \quad |\mathbf{v}_P(\Lambda)| = \sqrt{v_{PX}^2 + v_{PY}^2 + \Lambda^2} , \quad (2.14)$$

so that \mathbf{F} is continuous in \mathbf{v}_P and vanishes at $\mathbf{v}_P = \mathbf{0}$. Here we choose Λ as a sufficiently small number with dimensions of velocity. Note that $v_{PZ} = 0$ and thus the Z -component of \mathbf{F} is 0.

This completes the presentation of all the necessary equations for the analysis of the motion of tippe tops. We enumerate all these equations in Appendix A. We need further the initial conditions. When we play with a tippe top, we usually give it a rapid spin with its axis of symmetry nearly vertical. So let us choose the following initial conditions for θ and other angular velocities:

$$\begin{aligned} \theta_0 &= \theta(t=0) \quad \text{small} , & \dot{\theta}_0 &= \dot{\theta}(t=0) = 0 \\ \Omega_0 &= \Omega(t=0) = 0, \\ \dot{\psi}_0 &= \dot{\psi}(t=0) \quad \text{large} . \end{aligned} \quad (2.15)$$

We take $\theta_0 = 0.01 \sim 0.1$ rad and $\dot{\psi}_0 = 10 \sim 150$ rad/sec. Recall that the spin $n(t)$ is given by $n = \Omega \cos \theta + \dot{\psi}$, and thus we have $n_0 = n(t=0) = 10 \sim 150$ rad/sec. As for

the initial condition for the velocity of the center of mass O , we take

$$\mathbf{u}_0 = \mathbf{u}_O(t=0) = \mathbf{0} , \quad (2.16)$$

since we usually do not give a large translational motion to the tippe top at the beginning.

With the above initial conditions (2.15) and (2.16), we analyze the behaviors of the tippe top using three angular (2.6a-2.6c) and three translational (2.11a-2.11c) equations of motion, together with the knowledge of the frictional force, a modified version of the Coulomb law (2.14), and the velocities (2.8a-2.8c) and (2.9). When we perform simulations we use the adaptive Runge-Kutta method.

3 Gyroscopic balance condition

3.1 The variable ξ

We define a variable ξ as

$$\xi \equiv Cn - A\Omega \cos \theta . \quad (3.1)$$

In terms of ξ , the X - and Z - components of \mathbf{L} in (2.2) and Jellett's constant J , (2.7), are expressed, respectively, as

$$L_X = \xi \sin \theta, \quad L_Z = \xi \cos \theta + A \Omega , \quad (3.2)$$

$$J = -\xi a \sin^2 \theta + L_Z h(\theta) . \quad (3.3)$$

The condition $\xi=0$ has been introduced by MS [10] in their analysis of spinning hard-boiled eggs, and referred to as the GBC. They discovered that the GBC, $\xi=0$, is approximately satisfied for the spinning egg and, using this GBC, they resolved a long standing riddle: when a hard-boiled egg is spun sufficiently rapidly on a table with its axis of symmetry horizontal, the axis will rise from the horizontal to the vertical. We outline how MS found the GBC for the spinning egg [10]. The system of the spinning egg obeys essentially the same equations of motion as the case of

the tippe top, to be specific, Eqs. (2.3) and (2.10). The Y -component of (2.3) for the spinning egg is given by (2.6b), with the factor, $a \sin \theta$, being replaced by X_P . Because the secular change of θ is slow and thus $|\ddot{\theta}| \ll \Omega^2$, the term $A\ddot{\theta}$ can be neglected. Furthermore, in a situation where Ω^2 is sufficiently large so that the terms involving Ω in (2.6b) dominate the terms $-X_P N$ and $-h(\theta)F_X$, Eq. (2.6b) is reduced, in leading order, to $(Cn - A\Omega \cos \theta)\Omega \sin \theta = 0$. Hence, for $\sin \theta \neq 0$, we arrive at the condition $\xi = Cn - A\Omega \cos \theta = 0$.

The tippe top shows the similar behavior as the spinning egg. Then one may ask: does the GBC also hold for the tippe top? We will show that the answer is “partly no” and “partly yes”. “Partly no” means that the GBC is not satisfied initially. Tippe tops are usually spun with $\theta_0 \approx 0$, $\Omega_0 \approx 0$, and large $\dot{\psi}_0$ and, therefore, $n_0 \approx \dot{\psi}_0$ is large, from which we find that $\xi_0 = \xi(t=0) \approx Cn_0$ is large¹. Thus the GBC does not hold at the beginning. However, we will see later that the GBC does approximately hold whenever the tippe top rises, which is the meaning of “partly yes”. In fact, the argument of MS to derive the GBC for the spinning egg can also be applied to the tippe top. Thus in a situation where Ω is sufficiently large and for $\sin \theta \neq 0$, the GBC is expected to be satisfied. On the other hand, in the case of the spinning egg, the GBC is approximately satisfied initially. We start to spin an egg with its symmetry axis horizontal, that is, with $\theta_0 \approx \frac{\pi}{2}$, $\dot{\psi}_0 \approx 0$ and large Ω_0 . Hence we find $n_0 \approx 0$ and $\xi_0 \approx 0$ for the spinning egg.

We emphasize that the variable ξ initially takes a large positive value for the tippe top. But our numerical analysis will show that when a tippe top turns over, ξ soon makes a rapid transition from large positive values to negative values and starts to oscillate about a small negative value.

Before proceeding with a discussion of this transition of ξ , let us consider the consequences when the GBC is exactly satisfied for the tippe top.

¹In this paper we always take the initial spin velocity $\dot{\psi}_0$ about Oz to be positive and, therefore, ξ_0 is positive.

3.2 Consequences of the exact GBC

In a situation where Ω is sufficiently large and θ is not in the vicinity of 0 or π , the GBC is realized for the tippe top. Let us consider the case that the exact GBC, $\xi = 0$, is satisfied for the tippe top. Then, we have

$$J = L_Z h(\theta) , \quad (3.4)$$

from (3.3), and $L_Z = A\Omega$ from the second equation in (3.2). If the angular velocity Ω around the vertical axis is reduced and, therefore, L_Z decreases, Eq.(3.4) tells us that the height $h(\theta)$ of the center of mass from the table increases since J is a constant, which means the turning over of the tippe top. Differentiating both sides of (3.4) by time and using (2.4b) and (2.5c), we obtain a first-order ODE for θ ,

$$J\dot{\theta} = -F_Y h^2(\theta) . \quad (3.5)$$

We assume also that the Y -component of \mathbf{u}_O , the translational velocity of the center of mass O , in (2.9) is negligible in the first approximation as compared with that of $\mathbf{v}_{\text{rot}P}$, and we set $v_{PY} = v_{\text{rot}PY}$. We see that numerical simulation supports this assumption. Then, one can use Eq. (2.8b) and the GBC to eliminate n and Ω , and obtain v_{PY} as only a function of the dynamical variable θ as follows:

$$v_{PY} = \frac{J \sin \theta}{A h(\theta)} \left\{ a + R \left(\frac{A}{C} - 1 \right) \cos \theta \right\} . \quad (3.6)$$

Since the frictional force F_Y is proportional to v_{PY} , we obtain from Eqs.(3.5-3.6),

$$\dot{\theta} \propto \tilde{v}_{PY} \quad (3.7)$$

with a *positive* proportional coefficient and

$$\tilde{v}_{PY} = \sin \theta \left\{ a + R \left(\frac{A}{C} - 1 \right) \cos \theta \right\} . \quad (3.8)$$

Equation (3.7) implies that the change of θ is governed by the sign of \tilde{v}_{PY} . If \tilde{v}_{PY} is positive (negative), then θ will increase (decrease) with time. Therefore a close examination of the behavior of \tilde{v}_{PY} as a function of θ will be important ².

²A resemblance of (3.7) to a renormalization group equation which appears in quantum field theories for critical phenomena and high energy physics is emphasized in Sec. 5.

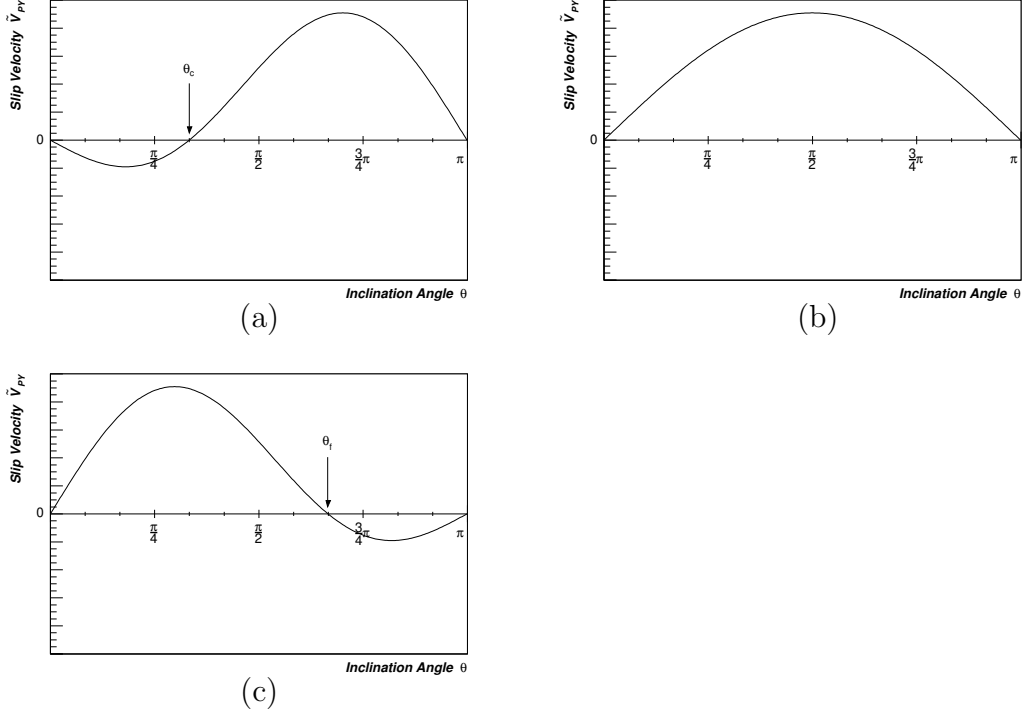


Figure 2: \tilde{V}_{PX} as a function of θ for tippe tops of (a) Group I with $\frac{a}{R} = 0.1$ and $\frac{A}{C} = 0.8$; (b) Group II with $\frac{a}{R} = 0.1$ and $\frac{A}{C} = 1$; (c) Group III with $\frac{a}{R} = 0.1$ and $\frac{A}{C} = 1.2$.

We observe from (3.8) that $\tilde{v}_{PY} = 0$ at $\theta = 0$ and π , since $\sin \theta = 0$ at these angles. Moreover, \tilde{v}_{PY} may vanish at an other angle, which is given by solving

$$a + R\left(\frac{A}{C} - 1\right) \cos \theta = 0. \quad (3.9)$$

Equation (3.9) has a solution for θ if $\frac{A}{C} < 1 - \frac{a}{R}$ or $1 + \frac{a}{R} < \frac{A}{C}$ and no solution otherwise. Accordingly, tippe tops are classified into three groups, depending on the values of $\frac{A}{C}$ and $\frac{a}{R}$: Group I with $\frac{A}{C} < 1 - \frac{a}{R}$; Group II with $1 - \frac{a}{R} < \frac{A}{C} < 1 + \frac{a}{R}$; and Group III with $1 + \frac{a}{R} < \frac{A}{C}$.

We now examine the behaviors of tippe tops belonging to each group.

(i) Group I $\left(\frac{A}{C} < 1 - \frac{a}{R}\right)$

Imagine that a familiar top consisting of a circular disk and a stem is located inside

of a hollow massless sphere. The stem is along the diameter of the sphere whose center does not coincide with the center of mass. This toy may belong to Group I. Figure 2 (a) shows a typical graph of \tilde{v}_{PY} for a tippe top of Group I. The graph crosses the line $\tilde{v}_P = 0$ at an angle

$$\theta_c = \cos^{-1} \left(\frac{a}{R(1 - \frac{A}{C})} \right) \quad \text{and} \quad 0 < \theta_c < \frac{\pi}{2}, \quad (3.10)$$

and \tilde{v}_{PY} is positive for $\theta_c < \theta < \pi$ but negative for $0 < \theta < \theta_c$. So, the angle θ_c is a *critical point*. If a tippe top of Group I is spun on a table with $\dot{\psi}_0 \approx 0$ and sufficiently large Ω_0 and with the initial angle $\theta_0 > \theta_c$, then θ will increase to π , which means that the body will eventually spin at $\theta = \pi$. In the case $\theta_0 < \theta_c$, we will see that the body spins at $\theta = 0$. Depending on the initial value θ_0 the body will spin at the end point $\theta = 0$ or π . Both ends are stable points. Usually we give a spin to the tippe top at a position with $\theta_0 \approx 0$. Spun at $\theta_0 \approx 0$, the tippe top of Group I does not turn over however large a spin it is given and will stay spinning at $\theta \approx 0$.

(ii) Group II $(1 - \frac{a}{R} < \frac{A}{C} < 1 + \frac{a}{R})$

Commercial tippe tops belong to Group II. A typical graph of \tilde{v}_{PY} for a tippe top of Group II is shown in Fig. 2 (b). We see that \tilde{v}_{PY} is positive for $0 < \theta < \pi$. Therefore, the end point at $\theta = 0$ is unstable while the other end at $\theta = \pi$ is a stable point. Once given a sufficiently large spin at $\theta_0 \approx 0$, the tippe top of Group II will turn over and spin at $\theta = \pi$. Actually, commercial tippe tops have stems. Thus for those tops the above statement is valid up to the angle when the stem touches the table.

(iii) Group III $(1 + \frac{a}{R} < \frac{A}{C})$

For an example of the tippe top of Group III, we may imagine a prolate spheroid put inside of a hollow massless sphere. The symmetric axis is along the diameter of the sphere and the mass distribution is nonuniform so that the center of mass is apart from the sphere's center. Figure 2 (c) shows a typical graph of \tilde{v}_{PY} for a tippe top of Group III. Similarly to the case of Group I the graph crosses the line $\tilde{v}_P = 0$ at an angle

$$\theta_f = \cos^{-1} \left(\frac{a}{R(1 - \frac{A}{C})} \right) \quad \text{and} \quad \frac{\pi}{2} < \theta_f < \pi. \quad (3.11)$$

In this case \tilde{v}_{PY} is positive for $0 < \theta < \theta_f$ and negative for $\theta_f < \theta < \pi$. So, both ends at $\theta = 0$ and π are unstable points, while the angle θ_f is a *fixed point*. When the body is spun sufficiently rapidly with the initial angle θ_0 anywhere, θ will approach the fixed point θ_f . Thus the tippe top of Group III, even though given a sufficiently large spin at $\theta_0 \approx 0$, will never turn over to $\theta = \pi$ but up to the angle θ_f .

Now it should be emphasized that the argument so far for the classification of tippe tops into three groups is based on the assumption that the GBC, $\xi = 0$, is exactly satisfied. It is very interesting to note that the above classification into three groups and its classificatory criteria totally coincide with those obtained by Hugenholtz [3] and Leutwyler [6], both of whom resorted to completely different arguments and methods. In fact, Hugenholtz considered the effect on the tippe top when a small frictional force is working during the uniform motion and reached the same conclusion. On the other hand, Leutwyler used Lagrangian formalism and searched for the minimum of energy for the tippe top under the constraint of Jellett's constant (2.7). Finally the behavior of the tippe top under the GBC was studied earlier by Sakai [15]. Unfortunately, his work was written in Japanese and is, therefore, not well known. The consequences derived in this subsection partly overlap with his results.

3.3 The behavior of the variable ξ

As stated before, the GBC is not satisfied initially for the tippe top. Actually, the initial value of ξ is large and positive. We have performed numerical computations to see the behaviors of ξ and θ in time t . Typical examples are shown in Figs. 3 and 4, where the scale of the left sides is for ξ normalized by the initial value ξ_0 , while the scale of the right sides is for θ in radian. Input parameters are for both cases

$$\begin{aligned} R &= 1.5 \text{ cm}, \quad a = 0.15 \text{ cm}, \quad M = 15 \text{ g}, \quad g = 980 \text{ cm/sec}^2, \\ A &= C = \frac{2}{5}MR^2, \quad \mu = 0.1, \quad \Lambda = 1 \text{ cm/sec}. \end{aligned} \quad (3.12)$$

For initial conditions we choose $n_0 = 100$ rad/sec, $\dot{\theta}_0 = \Omega_0 = 0$, and $\mathbf{u}_0 = \mathbf{0}$ for both cases, but we take $\theta_0 = 0.1$ rad for the simulation shown in Fig.3 and $\theta_0 = 0.01$ rad for the one in Fig.4. With these initial conditions we have $\xi_0 = Cn_0$ and

$J = \xi_0(R \cos \theta_0 - a)$. We show in Fig.5 the trajectories of slip velocity of the contact point P in the (v_{PX}, v_{PY}) space which are obtained from the above simulations with (a) $\theta_0 = 0.1$ and (b) $\theta_0 = 0.01$. The argument in section 3.2 tells us that a tippe top represented by the input parameters (3.12) is classified into Group II and, therefore, this tippe top would turn over up to an inverted position, $\theta = \pi$, when it is given a sufficiently large initial spin.

Also plotted in Figs.3 and 4 are the curves ξ_+ and ξ_- , the expressions of which are given below. Using Eqs.(3.2-3.3) and replacing Ω and L_Z with ξ , θ and J , we find that the X - and Y - components of the rotational equations (2.5a-2.5b) are rewritten as

$$\dot{\xi} \sin \theta = U(\xi, \theta, J) \dot{\theta} + h(\theta) F_Y, \quad (3.13a)$$

$$A\ddot{\theta} = -\frac{1}{Ah(\theta)} V(\xi, \theta, J) \sin \theta - h(\theta) F_X, \quad (3.13b)$$

with

$$U(\xi, \theta, J) = \frac{J - \xi(R \cos \theta - a)}{h(\theta)} - \xi \cos \theta, \quad (3.13c)$$

$$V(\xi, \theta, J) = \{J - \xi(R \cos \theta - a)\} \xi + AMgah(\theta), \quad (3.13d)$$

where we have set $N = Mg$. We see in Figs. 3 and 4, especially in the former, that θ changes while nutating. We also see that the inflection points of θ , where the condition $\ddot{\theta} = 0$ is satisfied, fall on a rather smooth curve about which θ nutates. At these inflection points of θ , the right-hand side (RHS) of Eq.(3.13b) vanishes. Here we note that, unless $\sin \theta \approx 0$, the second term $-h(\theta) F_X$ may be neglected as compared with the first term, since Fig.5 shows the smallness of v_{PX} . Then solving $V(\xi, \theta, J) = 0$ for ξ , we obtain

$$\xi_{\pm} = \frac{J \pm \sqrt{J^2 + 4AMg(R \cos \theta - a)(R - a \cos \theta)a}}{2(R \cos \theta - a)}. \quad (3.14)$$

We expect that at the inflection points of θ and if not $\sin \theta \approx 0$, ξ takes the values which are either on the curve ξ_+ or ξ_- . In the limit $(AMgR^2a)/J^2 \ll 1$ and $a \ll R$, which is true in these simulations, we have

$$\xi_+ \approx \frac{J}{R \cos \theta - a}, \quad \xi_- \approx -\frac{AMgaR}{J}, \quad (3.15)$$

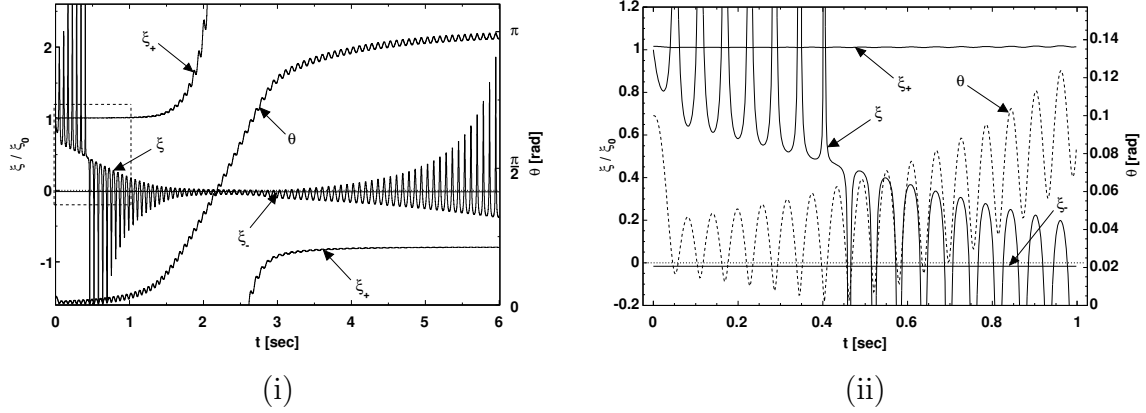


Figure 3: (i) Time evolution of the variable ξ and the inclination angle θ . Input parameters are $R=1.5$ cm, $a=0.15$ cm, $M=15$ g, $g=980$ cm/sec², $A=C=2/5MR^2$, $\mu=0.1$, $\Lambda=1$ cm/sec. Initial conditions are $\theta_0=0.1$ rad, $n_0=100$ rad/sec, $\dot{\theta}_0=\Omega_0=0$, $\mathbf{u}_0=\mathbf{0}$. The curves ξ_{\pm} are given by Eq.(3.14). (ii) Blow-up of the section surrounded by dashed lines in (i).

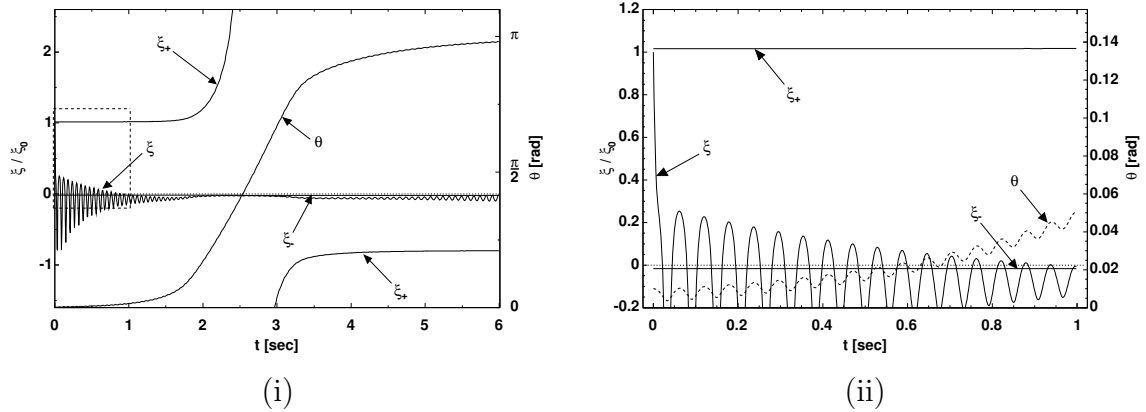


Figure 4: (i) Time evolution of the variable ξ and the inclination angle θ with an initial condition $\theta_0 = 0.01$ rad. Input parameters and other initial conditions are the same as in Figure 3. The curves ξ_{\pm} are given by Eq.(3.14). (ii) Blow-up of the section surrounded by dashed lines in (i).

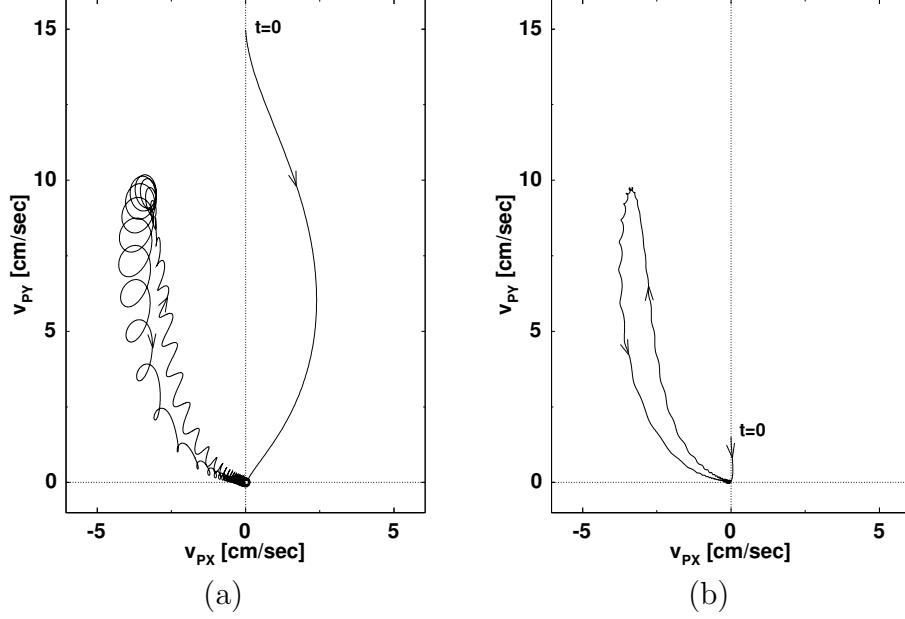


Figure 5: The trajectories of slip velocity of the contact point P in the (v_{PX}, v_{PY}) space which are obtained from (a) the simulation shown in Fig.3 with $\theta_0 = 0.1$ and (b) the one in Fig.4 with $\theta_0 = 0.01$.

and thus $\xi_-/\xi_0 \approx 0$.

Fig.3 shows the result of the simulation with an initial value $\theta_0 = 0.1$ rad. The variable ξ , starting from a large positive value $\xi_0 = Cn_0$, begins to fluctuate around the curve ξ_+ . The fluctuation of ξ becomes larger but ξ is still positive for a while. The inclination angle θ decreases rapidly from the initial value θ_0 and then starts to nutate. The amplitude of nutation becomes larger and the minimum value of θ decreases further. And at a certain point where $\theta \approx 0$, the fluctuation of ξ becomes so large that ξ takes negative values. Then ξ starts to fluctuate around the curve ξ_- and θ is going to increase while nutating. The fluctuation of ξ is getting smaller as θ is increasing, but it becomes large again when θ approaches π . We have observed in Fig.3 that the fluctuation of ξ around the curve ξ_+ at the beginning soon shifts to the one around the curve ξ_- . For this rapid transition of ξ , the simulation shows that

the system should pass through the phase where $\theta \approx 0$. When a simulation starts with a very small initial value θ_0 as in Fig.4, then ξ quickly moves to a fluctuation around the curve ξ_- .

Let us look more closely the behavior of ξ in Fig.3 at an early stage (to be specific, between $0 < t < 1$ sec). Recall $J = \xi_0(R \cos \theta_0 - a)$. Then Eq.(3.13c) gives $U(\xi, \theta, J)|_{t=0} = -\xi_0 \cos \theta_0$, which is large and negative. At the very beginning of time, Fig.5 (a) shows that $v_{PY}/|\mathbf{v}_P| \approx 1$, and thus we have $F_Y \approx -\mu Mg$. Also the term $\dot{\xi} \sin \theta$ on the left-hand side (LHS) of Eq.(3.13a) may be neglected in the leading order as compared with the $h(\theta)F_Y$ term, since $(d(\xi/\xi_0)/dt) \sin \theta \sim \sin \theta \times (1/\text{sec})$ and $\sin \theta$ is small, while $\mu MgR/\xi_0 \sim 2 \times (1/\text{sec})$. Hence we find from (3.13a),

$$\dot{\theta} \approx \frac{\mu M g h(\theta)}{U(\xi, \theta, J)} < 0, \quad \text{at the very beginning,} \quad (3.16)$$

which explains a rapid decrease of θ from an initial value θ_0 .

Along with the rapid decrease of θ , Fig.5 (a) shows that the slip velocity \mathbf{v}_P of the contact point P tends to vanish. Then, in this region where θ is small and $\mathbf{v}_P \approx \mathbf{0}$, the term $h(\theta)F_Y$ of the RHS of (3.13a) may be neglected while $U(\xi, \theta, J)$ is expressed as $U(\xi, \theta, J) \approx (\xi_0 - 2\xi)$. Hence Eq.(3.13a) is reduced to

$$\dot{\xi} \sin \theta = (\xi_0 - 2\xi)\dot{\theta}, \quad (3.17)$$

and its solution is given by

$$|2\xi - \xi_0| = \text{const.} \times \frac{1 + \cos \theta}{1 - \cos \theta}. \quad (3.18)$$

We observe in the simulation shown in Fig.3 that the behavior of ξ during the time $0.05 < t < 0.4$ sec is approximately described as

$$\frac{\xi}{\xi_0} \approx \frac{1}{2} + C_1 \frac{1 + \cos \theta}{1 - \cos \theta}, \quad (3.19)$$

with a positive constant C_1 . Although the term $h(\theta)F_Y$ has been neglected to derive (3.17), the small effect of the frictional force still remains and it produces the nutation of θ , which in turn gives ξ a fluctuating behavior around the curve ξ_+ according to (3.19). Along with nutation, the minimum value of θ further decreases and so the fluctuation of ξ is getting larger.

Then at a certain point (at $t \approx 0.45$ sec), the behavior of ξ shifts to the one which is, later on up to 1 sec, roughly described as

$$\frac{\xi}{\xi_0} \approx \frac{1}{2} - C_2 \frac{1 + \cos \theta}{1 - \cos \theta}, \quad (3.20)$$

with a positive constant C_2 , and ξ may take negative values. Actually ξ fluctuates rapidly between positive and negative values. Also, with the shift of the behavior of ξ , $U(\xi, \theta, J)$ turns to always take positive values. In this region, v_{PY} is small but positive on the average in time (see Fig.5 (a)). Now taking the time average of both sides of (3.13a), we see $\overline{\dot{\theta}}$, the time average of $\dot{\theta}$, is positive, since the LHS, $\overline{\dot{\xi} \sin \theta}$, may be neglected while $\overline{h(\theta)F_Y}$ is negative. Thus, from 0.45 sec to 1 sec, θ gradually increases while nutating. As θ is increasing, the effect of $\sin \theta$ on $\dot{\xi}$ in the LHS of (3.13a) gets weaker and the fluctuation of ξ becomes smaller. In the end ξ oscillates mildly about a negative value ξ_- .

When we start simulation with a very small initial value $\theta_0 = 0.01$ rad as in Fig.4, ξ quickly takes negative values and θ starts to increase. The fluctuations of ξ and θ are much smaller than those in Fig.3. With a smaller θ_0 , the center of mass O receives less recoil from the frictional force \mathbf{F} , which explains the smaller fluctuations for ξ and θ .

So far we have shown the result of the numerical analysis for a tippe top which belongs to Group II. Given a sufficiently large spin, the GBC for this tippe top, which is not fulfilled initially, will soon be satisfied approximately, and the body will start to turn over. Actually the GBC, $\xi = 0$, is modified to $\xi = \xi_m \equiv -AMgaR/J$ and $|\xi_m/\xi_0| \ll 1$. This modification has an only effect of shifting the positions of θ_c (3.10) and θ_f (3.11) slightly.

Empirically we know that when a given spin is not fast enough, the tippe top does not turn over and stays spinning with its stem up. Later in Sec. 4, we argue that there exists a critical value for the initial spin given to the tippe tops of Group II and III. If the initial spin is below this critical value, then even the tippe tops of Group II and III do not turn over. We have performed similar simulations as those in Figs. 3 and 4 with the same tippe top and the same initial conditions, except that the initial spins are below the critical value. In these simulations we find that ξ , starting from a positive ξ_0 , first fluctuates around the negative value ξ_- and then

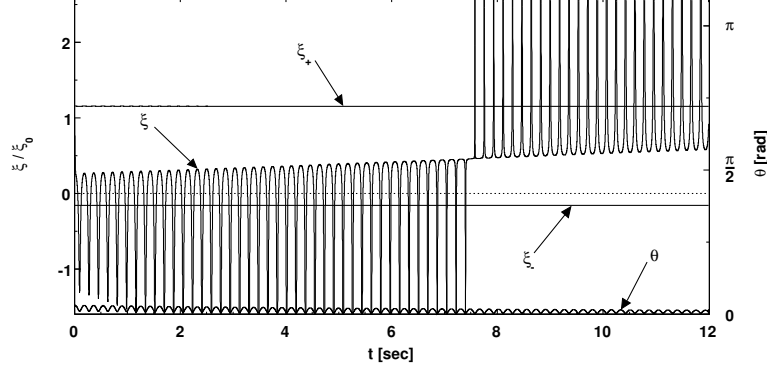


Figure 6: Time evolution up to 12 sec of the variable ξ and the inclination angle θ for a tippe top of Group II with an initial spin $n_0 = 30$ rad/sec. Input parameters and other initial conditions are the same as in Figure 3. The curves ξ_{\pm} are given by Eq.(3.14).

returns to positive values and fluctuates around ξ_+ , while the inclination angle θ remains approximately zero. A typical example is shown in Fig. 6, where input parameters and initial conditions are the same as in Fig. 3 (and thus the tippe top for this simulation belongs to Group II), except that the initial spin n_0 is 30 rad/sec. The critical value for the initial spin is given by n_1 in (4.18) below and we have $n_1 = 36$ rad/sec for this case.

We also performed simulations for the tippe tops of Group I, which are predicted to stay spinning at $\theta \approx 0$ however large a spin they are given. Plotted in Fig. 7 are the time evolution of ξ and θ for a tippe top belonging to Group I with initial spins (a) $n_0 = 100$ rad/sec and (b) $n_0 = 30$ rad/sec. Given a large initial spin (Fig. 7(a)), ξ for a tippe top of Group I stays positive and takes values very close to ξ_+ . But, with a small initial spin (Fig. 7(b)), ξ changes from a positive ξ_0 to negative and fluctuates around ξ_- for a while, and then back to positive values again. In both cases the tippe top stays spinning at $\theta \approx 0$.

For completeness we show, in Fig. 8, typical examples of the time evolution of ξ and θ for a tippe top belonging to Group III with initial spins, (a) $n_0 = 100$ rad/sec and (b) $n_0 = 15$ rad/sec. Input parameters and other initial conditions are

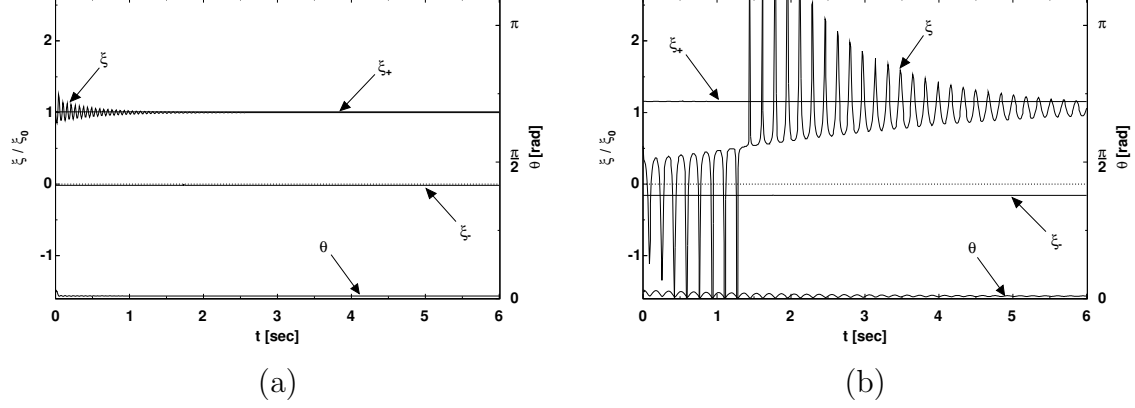


Figure 7: Time evolution of the variable ξ and the inclination angle θ for a tippe top of Group I with initial spins (a) $n_0 = 100$ rad/sec and (b) $n_0 = 30$ rad/sec. Input parameters are $R = 1.5$ cm, $a = 0.15$ cm (and thus $a/R = 0.1$), $M = 15$ g, $g = 980$ cm/sec², $A/C = 0.85$, $C = 2/5MR^2$, $\mu = 0.1$, $\Lambda = 1$ cm/sec. Other initial conditions are $\theta_0 = 0.1$ rad, $\dot{\theta}_0 = \Omega_0 = 0$, $\mathbf{u}_0 = \mathbf{0}$. The curves ξ_{\pm} are given by Eq.(3.14).

explained in the caption of Fig. 8. The critical value for the initial spin for the tippe top of Group III is given again by n_1 in (4.18) below and we have $n_1 = 23.5$ rad/sec for this simulation. When the initial spin n_0 is larger than the critical value n_1 (Fig. 8(a)), the variable ξ for a tippe top of Group III shows a similar behavior as the one presented in Fig. 3 for the tippe top of Group II. To be specific, ξ becomes small and fluctuates around the curve ξ_- while θ increases. Note that the tippe top of Group III never turns over to the inverted position, $\theta = \pi$. In the simulation of Fig. 8(a), θ goes up to the asymptotic angle θ_{asympt} , which is below the fixed point $\theta_f (= 2.21$ rad.) derived from (3.11). (See also the discussion on the plot in Fig. 10). Given a smaller initial spin than n_1 (Fig. 8(b)), ξ for a tippe top of Group III, starting from a positive ξ_0 , fluctuates around the negative value ξ_- and then becomes positive and fluctuates around ξ_+ , while θ remains approximately zero, a similar behavior as the one shown in Fig. 6 for the case of a tippe top of Group II with an insufficient initial spin.

From these numerical analyses we see that the behavior of ξ is closely related to the inversion phenomenon of the tippe top. As the tippe top turns over, simulation

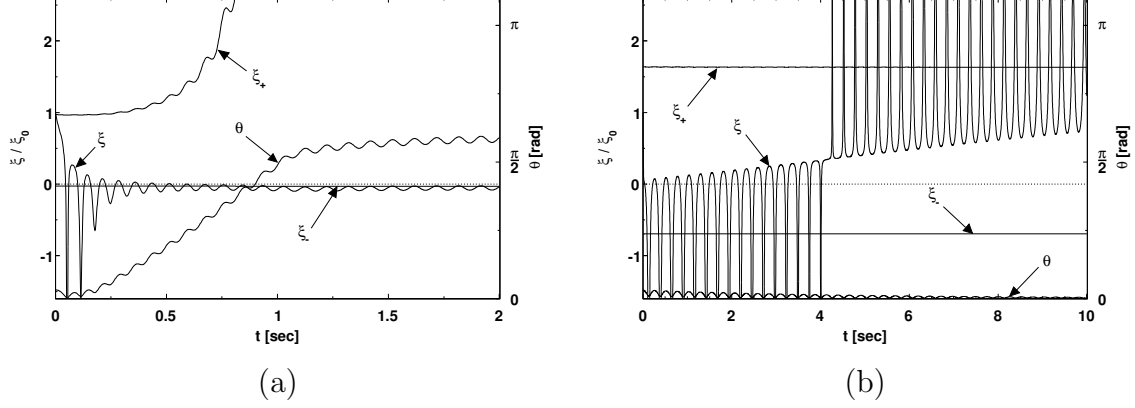


Figure 8: Time evolution of the variable ξ and the inclination angle θ for a tippe top of Group III with initial spins (a) $n_0 = 100$ rad/sec and (b) $n_0 = 15$ rad/sec. Input parameters are $R = 1.5$ cm, $a = 0.225$ cm (and thus $a/R = 0.15$), $M = 15$ g, $g = 980$ cm/sec², $A/C = 1.25$, $C = 0.8 \times (2/5)MR^2$, $\mu = 0.1$, $\Lambda = 1$ cm/sec. Other initial conditions are $\theta_0 = 0.1$ rad, $\dot{\theta}_0 = \Omega_0 = 0$, $\mathbf{u}_0 = \mathbf{0}$. The curves ξ_{\pm} are given by Eq.(3.14).

shows that ξ becomes small (in the sense $|\xi/\xi_0| \approx |\xi(R-a)/J| \ll 1$) and takes values close to $\xi_- \approx \xi_m$, which implies that the relation (3.4) is approximately satisfied. Conversely, when the relation (3.4) holds, it means that the center of mass of the tippe top goes up as L_Z decreases.

4 Stability and critical spin

4.1 Steady states

In Sec.3.2 we have studied the behaviors of the spinning tippe top when the gyroscopic balance condition $\xi = 0$ is exactly satisfied. The situation corresponds to the one in which the tippe top is given an infinitely large initial spin. Actually the initial spin given to the tippe top is finite and we know empirically that a tippe top with a small spin is stable and does not turn over. We will now consider how large

an initial spin should be for the tippe top to turn over. For that purpose we will study the steady states of the tippe top and examine their stability.

Actually the steady states (or the asymptotic states) of the tippe top and their stability were analyzed by Ebenfeld and Scheck [ES] [7]. They used the total energy of the spinning top as a Liapunov function. Then the steady states were found as solutions of constant energy. The stability or instability of these states was determined by examining whether the Liapunov function assumes a minimum or a maximum at these states under the constraint of Jellett's constant. The tippe top inversion was also analyzed recently by Bou-Rabee, Marsden and Romero [BMR] [9] as a dissipation-induced instability. BMR used the modified Maxwell-Bloch equations and an energy-momentum argument to determine the stability of the non-inverted and inverted states of the tippe top.

Here we take a different approach to this problem. And we discuss the stability of the steady states in terms of the initial spin velocity n given at the non-inverted position $\theta = 0$. Recently, Moffatt, Shimomura and Branicki [MSB] made a linear stability analysis of the spinning motion of spheroids [12]. They identified the steady states, and then discussed their stability and found the critical angular velocity needed for the rise of the body. In order to find the steady states of the spinning tippe top, we adopt the method taken by MSB for the case of spheroids. But for the stability analysis of the steady states, we develop a new stability criterion which is different from the ones used by ES, BMR and MSB.

Our approach to the stability problem of the tippe top is as follows. Once a steady state is known, the system is perturbed around the steady state. Particularly we focus our attention on the variable θ , which is perturbed to

$$\theta = \theta_s + \delta\theta , \tag{4.1}$$

where θ_s is a value at the steady state and $\delta\theta$ is a small quantity. Using the equations of motion, we obtain, under the linear approximation, a first-order ODE for $\delta\theta$ of the following form:

$$\delta\dot{\theta} = H\left(n_s, \Omega_s, \theta_s, \frac{A}{C}, \frac{a}{R}\right)\delta\theta , \tag{4.2}$$

where n_s and Ω_s are values taken at the steady state. Equation (4.2) implies that the change of $\delta\theta$ is governed by the sign of the function H . If H is positive (negative), $|\delta\theta|$ will increase (decrease) with time. Therefore, we conclude that *when H is negative (positive), then the state is stable (unstable)*. This is the criterion for stability of the steady state, which we will use in this paper. The stability criterion in this work is derived from an intuitive analysis of the equations of motion. We check in Appendices C and D that they are consistent with those derived by ES and BMR which are based on mathematically rigorous methods.

Superficially the above criterion (4.2) seems quite different from the one used by ES [7], but actually we have found that both are equivalent and, therefore, our results are consistent with theirs. In Appendix C we will show the equivalence of both criteria and that the stability conditions of the steady states which we will obtain coincide with the ones found by ES. After all, ES utilized the total energy (an integral form) [7], while we will use equations of motion (differential forms).

The criterion (4.2) for the stability of the tippe top also seems different from the ones used by BMR [9], which were derived from the tippe top modified Maxwell-Bloch equations. In order to obtain the stability criteria, both BMR and we linearize equations of motion about the steady states and use sliding friction, which is assumed to be an analytic function of the slip velocity, as the main mechanism behind tippe top inversion. Thus it is well expected that both criteria lead to the consistent results on the stability of the non-inverted and inverted states. (The stability of the intermediate states have not been analyzed yet by means of the modified Maxwell-Bloch equations). In Appendix D we will show that the expressions of the criteria provided in BMR become more transparent when they are rewritten in terms of the parameters and classification criteria used in this paper, and that they lead to the same stability conditions for the vertical spinning states which will be obtained later by using the criterion (4.2). Besides, although BMR did not mention, the classification of tippe tops into three groups, Group I, II, and III, is shown to be possible through the close examination of the criteria in BMR.

The steady states of the spinning motion of the tippe top are obtained from the equations of motion (2.6a-2.6c) and (2.11a-2.11c) by setting $\dot{\Omega} = \ddot{\theta} = \dot{\theta} = \dot{n} = \dot{u}_{OX} =$

$\dot{u}_{OY} = \dot{u}_{OZ} = 0$ [12]. Since we assume that the sliding friction (2.14), i.e., a modified version of Coulomb law³, is the only frictional force present, the energy equation

$$\frac{dE}{dt} = \mathbf{F} \cdot \mathbf{v}_P = -\mu N \frac{\mathbf{v}_P^2}{|\mathbf{v}_P(\Lambda)|} \quad (4.3)$$

shows that $\mathbf{v}_P = \mathbf{0}$ and $\mathbf{F} = \mathbf{0}$ at the steady states [12]. Thus we obtain for the steady states of the tippe top,

$$u_{OX} = 0, \quad (4.4a)$$

$$\Omega u_{OY} = 0, \quad (4.4b)$$

$$\Omega(Cn - A\Omega \cos \theta) \sin \theta + Mga \sin \theta = 0, \quad (4.4c)$$

$$u_{OY} + \{R(n - \Omega \cos \theta) + a\Omega\} \sin \theta = 0, \quad (4.4d)$$

where $N = Mg$ and the velocity equations (2.8a-2.8b) and (2.9) have been used. The solutions for Eqs.(4.4a-4.4d) are:

i) Vertical spin state at $\theta = 0$:

$$u_{OX} = u_{OY} = 0, \quad \theta = 0, \quad n \text{ arbitrary}, \quad \Omega \text{ undefined}, \quad (4.5)$$

which is a spinning state about the axis of symmetry with the center of mass below the sphere' center.

ii) Vertical spin state at $\theta = \pi$:

$$u_{OX} = u_{OY} = 0, \quad \theta = \pi, \quad n \text{ arbitrary}, \quad \Omega \text{ undefined}, \quad (4.6)$$

which is an overturned spinning state about the axis of symmetry with the center of mass above the sphere' center.

iii) Intermediate states:

$$u_{OX} = u_{OY} = 0, \quad 0 < \theta < \pi, \quad (4.7a)$$

$$\Omega(Cn - A\Omega \cos \theta) + aMg = 0, \quad (4.7a)$$

$$R(n - \Omega \cos \theta) + a\Omega = 0. \quad (4.7b)$$

³Recall that the exact Coulomb friction (2.13) is non-analytic at $\mathbf{v}_P = \mathbf{0}$ and a nonlinear friction law that would not appear in the linear approximation [5].

The elimination of n from (4.7a) and (4.7b) gives

$$\Omega^2 = \frac{Mga}{(A - C) \cos \theta + C \frac{a}{R}} . \quad (4.8)$$

The necessary (but not sufficient) condition for the existence of such states is

$$\left(\frac{A}{C} - 1 \right) \cos \theta + \frac{a}{R} > 0 . \quad (4.9)$$

Recall (3.9) which was used for the classification of tippe tops into three groups in Sec. 3.2. Thus, intermediate states may exist at $\theta > \theta_c = \cos^{-1} \left(\frac{a}{R(1 - \frac{A}{C})} \right)$ for the tippe top of Group I ($\frac{A}{C} < 1 - \frac{a}{R}$), at θ between 0 and π for Group II ($1 - \frac{a}{R} < \frac{A}{C} < 1 + \frac{a}{R}$), and at $\theta < \theta_f = \cos^{-1} \left(\frac{a}{R(1 - \frac{A}{C})} \right)$ for Group III ($1 + \frac{a}{R} < \frac{A}{C}$).

There appear, in total, three categories of steady states for a loaded sphere version of the tippe top.

4.2 Stability analysis of the steady states

The turnover of the tippe top is associated with the effect of the sliding friction (with a coefficient μ) at the point of contact P . Near the steady states, we know that $\mathbf{v}_P \approx \mathbf{0}$, which is equivalent to the situation where $\mu \approx 0$. Thus for the stability analysis of the steady states, we consider the limiting case of $\mu \ll 1$ [12]. Since we expect $\frac{d}{dt} \sim \mathcal{O}(\mu)$ near the steady states, we have $\dot{\theta} \sim \mathcal{O}(\mu)$ and $\ddot{\theta} \sim \mathcal{O}(\mu^2)$. Eq.(2.8b) shows $v_{\text{rot}PY} \sim \mathcal{O}(1)$, which leads to $v_{PY} \sim \mathcal{O}(1)$ and, hence, $F_Y \sim \mathcal{O}(\mu)$. Then (2.11b) gives $u_{OX} \sim \mathcal{O}(\mu)$, and $v_{PX} \sim \mathcal{O}(\mu)$ from (2.8a) and (2.9), and thus we have $F_X \sim \mathcal{O}(\mu^2)$ and $u_{OY} \sim \mathcal{O}(\mu^2)$.

The above order estimation in μ near the steady states leads to the primary balance in (2.6b) which holds at leading order in μ [12],

$$\Omega(Cn - A\Omega \cos \theta) + aMg = 0 . \quad (4.10)$$

Note that with a sufficiently large Ω , Eq.(4.10) reduces to $\xi = Cn - A\Omega \cos \theta = 0$, the GBC.

4.2.1 Stability of the vertical spin state at $\theta = 0$

The angle θ is perturbed from $\theta = 0$, and we take $\theta = \delta\theta \ll 1$. In the linear approximation we may take $n = \text{const.}$, since Eq.(2.6c) implies that \dot{n} is quadratic in small quantities (note $F_Y \sim \mathcal{O}(\mu)$). With $\cos\delta\theta = 1$, the primary balance (4.10) gives

$$\Omega = \frac{1}{2A} \left\{ Cn \pm \sqrt{(Cn)^2 + 4AMga} \right\} . \quad (4.11)$$

In this approximation Ω is also a constant. Then Eq.(2.6a) gives

$$\delta\dot{\theta} = \frac{R-a}{2A\Omega - Cn} \mu M g \frac{v_{PY}}{|\mathbf{v}_P(\Lambda)|} , \quad (4.12)$$

and we may take

$$v_{PY} = \{R(n - \Omega) + a\Omega\} \delta\theta, \quad (4.13)$$

since $u_{OY} \sim \mathcal{O}(\mu^2)$. Hence, we require for the stability at $\theta = 0$

$$\frac{R(n - \Omega) + a\Omega}{2A\Omega - Cn} < 0 . \quad (4.14)$$

Using the expressions of both “+” and “−” solutions for Ω in (4.11), the above condition is rewritten as

$$\pm \left(\frac{2AR}{R-a} - C \right) n < \sqrt{(Cn)^2 + 4AMga} , \quad (4.15)$$

which gives

$$n^2 \left\{ \frac{A}{C} - \left(1 - \frac{a}{R}\right) \right\} < \frac{Mga}{C} \left(1 - \frac{a}{R}\right)^2 . \quad (4.16)$$

It is easily seen that the requirement (4.16) is always satisfied for any spin velocity n by the tippe top of Group I ($\frac{A}{C} < 1 - \frac{a}{R}$). As for the tippe top of Group II or III with $\frac{A}{C} > \left(1 - \frac{a}{R}\right)$, the requirement (4.16) is rewritten as

$$n^2 < \frac{Mga}{C \left\{ \frac{A}{C} - \left(1 - \frac{a}{R}\right) \right\}} \left(1 - \frac{a}{R}\right)^2 = n_1^2 . \quad (4.17)$$

The stability of the vertical spin state at $\theta = 0$ is summarized as follows: For the tippe top of Group I with $\frac{A}{C} < (1 - \frac{a}{R})$, the spinning state at $\theta = 0$ is stable for any spin n , while for the tippe top of Group II or III with $\frac{A}{C} > (1 - \frac{a}{R})$ we require $n < n_1$ for its stability. In other words, the tippe top of Group II or III becomes unstable at $\theta = 0$ if

$$n(\theta = 0) > n_1 = \sqrt{\frac{Mga}{C\{\frac{A}{C} - (1 - \frac{a}{R})\}}} \left(1 - \frac{a}{R}\right) \quad (4.18)$$

4.2.2 Stability of the vertical spin state at $\theta = \pi$

A similar analysis can be made for the stability of the spinning state at $\theta = \pi$. Now put $\theta = \pi - \delta\theta'$ with $\delta\theta' \ll 1$. Again we may take $n = \text{const.}$, but note that n may be negative near $\theta = \pi$. With $\cos\theta = -1$, the primary balance (4.10) gives

$$\Omega = \frac{1}{2A} \left\{ -Cn \pm \sqrt{(Cn)^2 - 4AMga} \right\} . \quad (4.19)$$

In order for Ω to have a real solution, we require

$$|n| > \frac{2\sqrt{AMga}}{C} = n_2 . \quad (4.20)$$

For $|n| < n_2$, the spin is insufficient to overcome the effect of gravity and the orientation becomes unstable [12].

With $\dot{\Omega} = 0$, Eq. (2.6a) gives

$$\delta\dot{\theta}' = -\frac{R+a}{2A\Omega + Cn} \mu Mg \frac{v_{PY}}{|\mathbf{v}_P(\Lambda)|} , \quad (4.21)$$

and we may take,

$$v_{PY} = \{R(n + \Omega) + a\Omega\} \delta\theta' . \quad (4.22)$$

Hence we require for the stability at $\theta = \pi$,

$$\frac{R(n + \Omega) + a\Omega}{2A\Omega + Cn} > 0 . \quad (4.23)$$

Using the expressions of both “+” and “-” solutions for Ω in (4.19), the above condition gives

$$n^2 \left\{ \left(1 + \frac{a}{R}\right) - \frac{A}{C} \right\} > \frac{Mga}{C} \left(1 + \frac{a}{R}\right)^2. \quad (4.24)$$

First, the requirement (4.24) is never satisfied by the tippe top of Group III ($\frac{A}{C} > 1 + \frac{a}{R}$). So the tippe top of Group III is unstable at $\theta = \pi$. Actually it never turns over to the position with $\theta = \pi$. For the tippe top of Group I or II which satisfies $\frac{A}{C} < (1 + \frac{a}{R})$, the requirement (4.24) becomes

$$n^2 > \frac{Mga}{C \left\{ \left(1 + \frac{a}{R}\right) - \frac{A}{C} \right\}} \left(1 + \frac{a}{R}\right)^2 = n_3^2. \quad (4.25)$$

Note that $n_3^2 \geq n_2^2$.

The stability of the vertical spin state at $\theta = \pi$ is summarized as follows: For the tippe top of Group III ($1 + \frac{a}{R} < \frac{A}{C}$), the spinning state at $\theta = \pi$ is unstable for any spin n , while for the tippe top of Group I or II with $\frac{A}{C} < (1 + \frac{a}{R})$, the state at $\theta = \pi$ is stable if

$$|n(\theta = \pi)| > \sqrt{\frac{Mga}{C \left\{ \left(1 + \frac{a}{R}\right) - \frac{A}{C} \right\}}} \left(1 + \frac{a}{R}\right) = n_3. \quad (4.26)$$

4.2.3 Stability of the intermediate state

We have learned in Sec.4.2.1 that the spinning state of Group I at $\theta = 0$ is stable. We also know from the discussion in Sec.4.1 that the intermediate steady states of Group I, if they exist, must occur at $\theta > \theta_c = \cos^{-1} \left(\frac{a}{R(1 - \frac{A}{C})} \right)$. This implies that the spinning motion of Group I near $\theta = 0$ does not shift to a possible intermediate steady state. On the other hand, the tippe tops of Group II and III become unstable at $\theta = 0$ when they are spun with a sufficiently large initial spin $n(\theta = 0) > n_1$, where n_1 is given by (4.18), and they will start to turn over. Here we are interested in the intermediate steady states of the tippe top which are reached from the initial spinning position near $\theta = 0$. Therefore, in this subsection, we focus on the possible steady states only for the tippe tops of Group II and III, and examine their stability.

The Jellett's constant given by (2.7) or (3.3) is rewritten as

$$J = Cn(R \cos \theta - a) + A\Omega R \sin^2 \theta . \quad (4.27)$$

Now Eqs.(4.7a) and (4.7b) and the above expression of J completely determine the intermediate steady states. They are derived by solving

$$\kappa \left[\left(\frac{A}{C} - 1 \right) \cos \theta + \frac{a}{R} \right] = \left\{ \left(\cos \theta - \frac{a}{R} \right)^2 + \frac{A}{C} \sin^2 \theta \right\}^2 , \quad (4.28)$$

where

$$\kappa = \frac{J^2}{MgaCR^2} . \quad (4.29)$$

Define the following function:

$$F(x) = \frac{f_2(x)}{f_1(x)} , \quad (4.30)$$

where $x = \cos \theta$ and

$$f_1(x) = \left(\frac{A}{C} - 1 \right) x + \frac{a}{R} , \quad (4.31a)$$

$$f_2(x) = \left\{ \left(x - \frac{a}{R} \right)^2 + \frac{A}{C} (1 - x^2) \right\}^2 . \quad (4.31b)$$

Then, Eq.(4.28) is rewritten as

$$F(x) = \kappa . \quad (4.32)$$

Since $f_2'(x) = -4\sqrt{f_2(x)}f_1(x)$, we obtain

$$F'(x) = -4\sqrt{f_2(x)} - \frac{f_2(x)}{[f_1(x)]^2} \left(\frac{A}{C} - 1 \right) , \quad (4.33a)$$

$$F''(x) = \frac{2}{[f_1(x)]^3} \left\{ \left([f_1(x)]^2 + \left(\frac{A}{C} - 1 \right) \sqrt{f_2(x)} \right)^2 + 3[f_1(x)]^4 \right\} > 0 . \quad (4.33b)$$

The condition for the initial spin $n(\theta = 0) > n_1$ means $J > Cn_1(R - a)$. Using (4.18), we find $\kappa > (1 - \frac{a}{R})^4 / (\frac{A}{C} - 1 + \frac{a}{R})$, which leads to $\kappa > F(1)$. So we are looking for solutions of $F(x) = \kappa$ with $\kappa > F(1)$.

(i) Group II $(1 - \frac{a}{R} < \frac{A}{C} < 1 + \frac{a}{R})$

When $1 \leq \frac{A}{C} < (1 + \frac{a}{R})$, $F'(x) < 0$ and $F(x)$ is a monotonically decreasing function for $-1 \leq x \leq 1$. Hence, there is one and only one solution of $F(x) = \kappa$ at x_s between -1 and 1 , provided $F(1) < \kappa < F(-1)$. Otherwise, there is no solution, which means that there exists no intermediate steady state. Expressing J with the initial spin at $\theta=0$ as $J = Cn(\theta=0)(R-a)$, we find that the condition $\kappa < F(-1)$ gives

$$n(\theta=0) < \sqrt{\frac{Mga}{C\{(1 + \frac{a}{R}) - \frac{A}{C}\}}} \frac{(1 + \frac{a}{R})^2}{(1 - \frac{a}{R})} = n_4. \quad (4.34)$$

Thus, in the case $1 \leq \frac{A}{C} < (1 + \frac{a}{R})$, one intermediate steady state exists at x_s , provided that

$$n_1 < n(\theta=0) < n_4. \quad (4.35)$$

We know $F''(x) > 0$ from (4.33b), and so $F(x)$ is concave upward for $-1 \leq x \leq 1$. If $(1 - \frac{a}{R}) < \frac{A}{C} < 1$, then $F(x)$ may have a local minimum at a certain x between -1 and 1 . Recall that we are looking for the steady states which are reached from the position near $\theta = 0$ and that the requirement for this is $\kappa > F(1)$. Hence, for the existence of such a steady state we need

$$F(-1) > F(1) \quad \text{and} \quad F(-1) > \kappa > F(1). \quad (4.36)$$

The first condition $F(-1) > F(1)$ gives

$$\frac{A}{C} > 1 - \frac{a}{R} \frac{(1 + \frac{a}{R})^4 - (1 - \frac{a}{R})^4}{(1 + \frac{a}{R})^4 + (1 - \frac{a}{R})^4} \equiv r_c, \quad (4.37)$$

and the second one $F(-1) > \kappa > F(1)$ leads to $n_1 < n(\theta=0) < n_4$. Some tippe tops of Group II with $\frac{A}{C} < 1$ satisfy $F'(1) > 0$ as well as the conditions (4.36), and thus $r_c < \frac{A}{C} < 1$. For such tippe tops, the corresponding $F(x)$ has a local minimum between x_d and 1 , where x_d is a solution of $F(x_d) = F(1)$. These tippe tops, therefore, have one intermediate steady state at x_s between -1 and x_d when the condition $n_1 < n(\theta=0) < n_4$ is satisfied. See the discussion of case (c) in Fig.9.

For the tippe tops of Group II with $(1 - \frac{a}{R}) < \frac{A}{C} < r_c$, there exists no intermediate state. We will see later, in the discussion of case (d) in Fig.9, that these tippe tops will turn over to $\theta = \pi$ once given a spin $n(\theta = 0) > n_1$, since $F(-1) < F(1)$ and, hence, $n_1 > n_4$ for these tops.

(ii) Group III $(1 + \frac{a}{R} < \frac{A}{C})$

Since $f_1(x)$ should be positive, the allowed region of x is $x_f < x \leq 1$ with $x_f = \frac{a}{R(1 - \frac{A}{C})}$. Eq.(4.33a) together with $(\frac{A}{C} - 1) > 0$ shows that $F(x)$ is a monotonically decreasing function for $x_f < x \leq 1$. Note that $F(x)$ positively diverges when x approaches x_f from larger x . Hence, once $\kappa > F(1)$ is satisfied, $F(x) = \kappa$ has one and only one solution at x_s such that $x_f < x_s < 1$. In other words, one intermediate steady state always exists at $\theta_s (= \cos^{-1} x_s)$ between 0 and $\theta_f (= \cos^{-1} x_f)$ for the tippe top of Group III, if the condition $n(\theta = 0) > n_1$ is satisfied. When $n(\theta = 0)$ gets larger, the angle θ_s gets closer to θ_f but never crosses θ_f . In order for θ_s to reach θ_f , $n(\theta = 0)$ should be infinite.

Now we know that there exists an intermediate steady state for the tippe top of Group II with property $r_c < \frac{A}{C} < 1 + \frac{a}{R}$, when $n(\theta = 0)$ satisfies $n_1 < n(\theta = 0) < n_4$. Also there is an intermediate steady state for the tippe top of Group III with $(1 + \frac{a}{R}) < \frac{A}{C}$ if $n(\theta = 0) > n_1$. Let $(n_s, \Omega_s, \theta_s)$ represent such a steady state so that $(n_s, \Omega_s, \theta_s)$ are related by Eqs.(4.7a) and (4.7b), and suppose this state to be perturbed to

$$n = n_s + \delta n, \quad \Omega = \Omega_s + \delta \Omega, \quad \theta = \theta_s + \delta \theta. \quad (4.38)$$

Noting that $\dot{\theta}_s = 0$ and $F_Y|_s = 0$, we find that the perturbed state satisfies

$$\delta \dot{\theta} = -\frac{\mu M g}{\Lambda} \frac{R^2 \sin^2 \theta_s}{C \left\{ S_s^2 + \left(\frac{A}{C} \sin \theta_s \right)^2 \right\}} D(x_s) \delta \theta, \quad (4.39)$$

where

$$D(x_s) = 4 \left[f_1(x_s) \right]^2 + \left(\frac{A}{C} - 1 \right) \sqrt{f_2(x_s)}. \quad (4.40)$$

The details of the derivation of (4.39) are given in Appendix B.

If $\frac{A}{C} > 1$, then $D(x_s) > 0$. Also when $r_c < \frac{A}{C} < 1$, we find that $D(x_s)$ is still positive (see Appendix B). Thus we observe from (4.39) that $\delta \dot{\theta} \propto \delta \theta$ with a

negative constant at the intermediate steady state, which means that this state is indeed stable.

Finally it is emphasized that the spinning state of the tippe top of Group I is stable at $\theta=0$ and the top will not turn over from the position near $\theta=0$. On the other hand, the tippe top of Group III, when given a sufficiently large spin near the position $\theta=0$, will tend to turn over and approach the steady state at θ_s but never up to the inverted position at $\theta = \pi$.

4.3 Critical spin for inversion of the tippe top of Group II

The tippe top of Group II will turn over to the inverted position at $\theta=\pi$ when it is given a sufficient initial spin. Let us estimate the critical value n_c so that the spinning top with $n(\theta=0) > n_c$ reaches the inverted position.⁴ Recall that Jellett's constant (4.27) is invariant during the turnover from $\theta = 0$ to $\theta = \pi$. From the relation $Cn(\theta=0)(R-a) = Cn(\theta=\pi)(-R-a)$, we obtain

$$n(\theta = \pi) = -\frac{R-a}{R+a}n(\theta = 0) . \quad (4.41)$$

We already know that we need $|n(\theta=\pi)| > n_3$ for the stability at $\theta=\pi$, where n_3 is given in (4.26). Thus we find

$$n(\theta = 0) > \sqrt{\frac{Mga}{C\{(1+\frac{a}{R})-\frac{A}{C}\}}} \frac{\left(1+\frac{a}{R}\right)^2}{\left(1-\frac{a}{R}\right)} = n_4 . \quad (4.42)$$

Also from the instability condition of the tippe top of Group II at $\theta=0$, we need $n(\theta=0) > n_1$, where n_1 is given by (4.18). Hence the condition for the tippe top of Group II to turn over up to $\theta = \pi$ is that the initial spin $n(\theta=0)$ should be larger than both n_4 and n_1 . In fact, we observe $n_4 > n_1$ for the tippe top with

⁴ The idea is borrowed from Ref.[12], where MSB estimated the critical angular velocity above which a uniform prolate spheroid will rise to the vertical state under the assumption of the GBC and thus the existence of Jellett's constant.

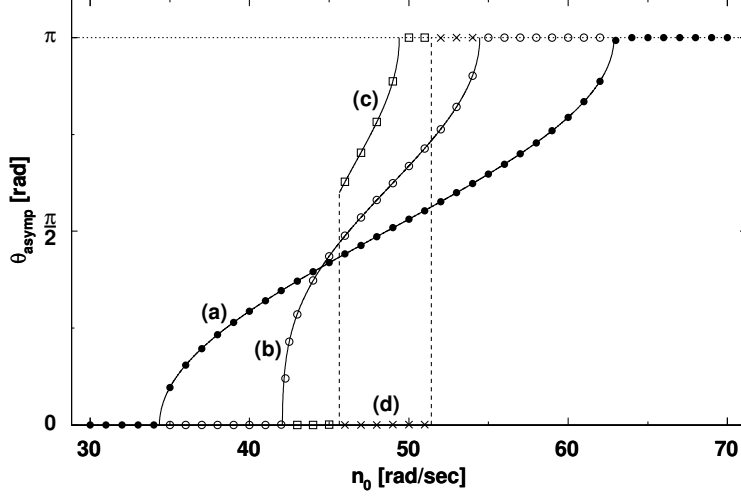


Figure 9: The asymptotic value θ_{asympt} as a function of the initial spin velocity n_0 for tippe tops of Group II with various values of $\frac{A}{C}$ and $\frac{a}{R}$; (a) the one with $\frac{A}{C} = 1$ and $\frac{a}{R} = 0.15$; the others have $\frac{A}{C} = 0.95$ but different $\frac{a}{R}$ such as (b) $\frac{a}{R} = 0.15$, (c) $\frac{a}{R} = 0.125$ and (d) $\frac{a}{R} = 0.1$.

$r_c < \frac{A}{C} < 1 + \frac{a}{R}$, while $n_4 < n_1$ for the tippe top with $1 - \frac{a}{R} < \frac{A}{C} < r_c$, where r_c is given by (4.37). Therefore, we obtain

$$n_c = \begin{cases} n_4, & \text{for } r_c < \frac{A}{C} < 1 + \frac{a}{R}, \\ n_1, & \text{for } 1 - \frac{a}{R} < \frac{A}{C} < r_c. \end{cases} \quad (4.43)$$

4.4 Numerical analysis

We now study the time evolution of the inclination angle θ from a spinning position near $\theta = 0$. Simulations are made with various values of $\frac{A}{C}$ and $\frac{a}{R}$, changing the input parameters A and a . Other input parameters are the same as those given in (3.12). Initial conditions are $\theta_0 = 0.01$ rad, $\dot{\theta}_0 = \Omega_0 = 0$, and $\mathbf{u}_0 = \mathbf{0}$, and the initial value of the spin velocity n_0 is varied. Since we have chosen a very small θ_0 , we may consider n_0 as $n(\theta=0)$.

Figure 9 shows the asymptotic (final) angle of inclination, θ_{asympt} , as a function

of n_0 for several types of tippe tops of Group II with different values of $\frac{A}{C}$ and $\frac{a}{R}$; (a) the one with $\frac{A}{C} = 1$ and $\frac{a}{R} = 0.15$; the others have $\frac{A}{C} = 0.95$ but different $\frac{a}{R}$ such as (b) $\frac{a}{R} = 0.15$, (c) $\frac{a}{R} = 0.125$, and (d) $\frac{a}{R} = 0.1$. The asymptotic angle θ_{asympt} may be 0 or π , or θ_s , the angle of a possible intermediate steady state.

The symbols \bullet , \circ , \diamond and \times represent the results for the tippe tops (a), (b), (c) and (d), respectively, and the thin solid curves (a), (b) and (c) are the trajectories obtained by solving (4.28). We observe that the numerical results fall on the predicted curves. The values of $n_1(n_4)$, in units of rad/sec, for the tops (a), (b), (c) and (d) are 34.4(62.9), 42.1(54.5), 45.7(49.4) and 51.4(44.4), respectively. In each case we see that the spinning state near $\theta=0$ is stable when $n_0 < n_1$. Once n_0 gets larger than n_1 , the state becomes unstable and the tippe top turns over up to the asymptotic angle θ_{asympt} . For the tippe tops (a) and (b) the values of θ_{asympt} grow with n_0 from 0 to π . On the other hand, the tippe top (c) satisfies $r_c < \frac{A}{C} < 1$ with $r_c = 0.94$, and thus the intermediate steady state exists only at $\theta_s (= \theta_{\text{asympt}})$ with $\theta_d < \theta_s < \pi$, where θ_d is a solution of $F(\cos \theta_d) = F(1)$. We find $\theta_d = 1.89$. Thus when n_0 gets larger than n_1 for the case of the tippe top (c), the asymptotic angle θ_{asympt} jumps from 0 to θ_d . When $n_0 > n_4$, $\theta_{\text{asympt}} = \pi$ for the tops (a), (b) and (c). In the case of the tippe top (d), we find $r_c = 0.96$ and thus $\frac{A}{C} < r_c$, which leads to $n_1 > n_4$. Therefore, there is no intermediate steady state, and the asymptotic angle θ_{asympt} is 0 or π depending on $n_0 \lessgtr n_1$.

We plot in Fig.10 the asymptotic angle θ_{asympt} as a function of n_0 for the tippe tops of Group III; (a) with $\frac{A}{C} = 1.25$ and $\frac{a}{R} = 0.025$ and (b) with $\frac{A}{C} = 1.25$ and $\frac{a}{R} = 0.15$. The symbols \bullet and \circ represent the results of simulation for the tippe tops (a) and (b), respectively, and the thin solid curves (a) and (b) are the trajectories obtained by solving (4.28). We observe again that the numerical results on θ_{asympt} for both tops (a) and (b) fall on the predicted curves. The values of n_1 for the tops (a) and (b) are 13.3 and 23.5 rad/sec, respectively. In both cases the spinning position near $\theta = 0$ is stable when n_0 is below n_1 . Above n_1 , the value of θ_{asympt} grows with n_0 and approaches the fixed point θ_f . The values of θ_f for the tops (a) and (b) are 1.67 and 2.21 rad, respectively.

For simulations we have used a modified version of the Coulomb friction \mathbf{F} given

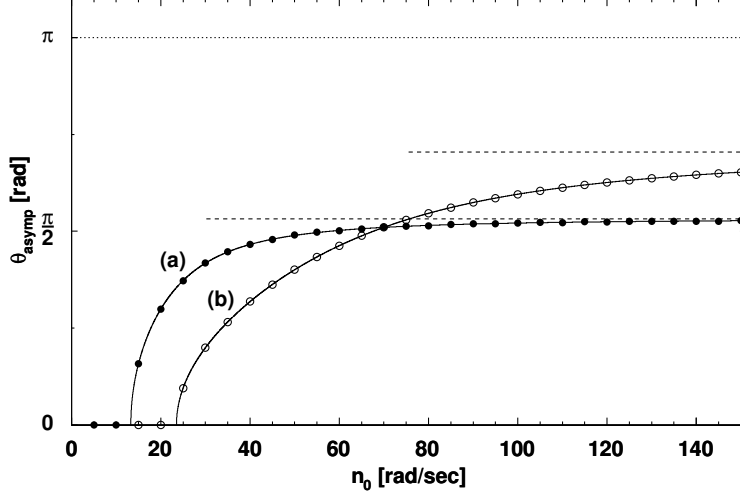


Figure 10: The asymptotic value θ_{asympt} as a function of the initial spin velocity n_0 for tippe tops of Group III: (a) with $\frac{A}{C} = 1.25$ and $\frac{a}{R} = 0.025$; and (b) with $\frac{A}{C} = 1.25$ and $\frac{a}{R} = 0.15$.

in (2.14). The value θ_{asympt} is not affected by the strength of the coefficient μ . The strength of μ instead has an effect on the rate of rising of the tippe top. If we use another form than (2.14) for the sliding friction, and moreover, it is expressed as a continuous function of \mathbf{v}_P and vanishes at $\mathbf{v}_P = \mathbf{0}$, then we still expect that we get the same numerical results on θ_{asympt} vs. n_0 as shown in Fig.9 and Fig.10. This is due to the observation that the numerical value θ_{asympt} has fallen on the predicted curves which are derived from (4.28) and that we have obtained (4.28) using the property of \mathbf{F} which vanishes at the steady states together with \mathbf{v}_P .

Figure 11 shows the time evolution of the inclination angle θ for a tippe top of Group II from a spinning position near $\theta = 0$ for various values of the initial spin velocity n_0 . Input parameters and initial conditions are the same as before and we take $\frac{A}{C} = 1$ and $\frac{a}{R} = 0.15$. The asymptotic angles θ_{asympt} which will be reached are 0, 0.92, 1.67, 2.49, π and π rad for $n_0 = 30, 40, 50, 60, 70$ and 80 rad/sec, respectively. Simulations with a modified version of the Coulomb friction (2.14) show that the larger value of n_0 is given, the faster the rate of rising becomes.

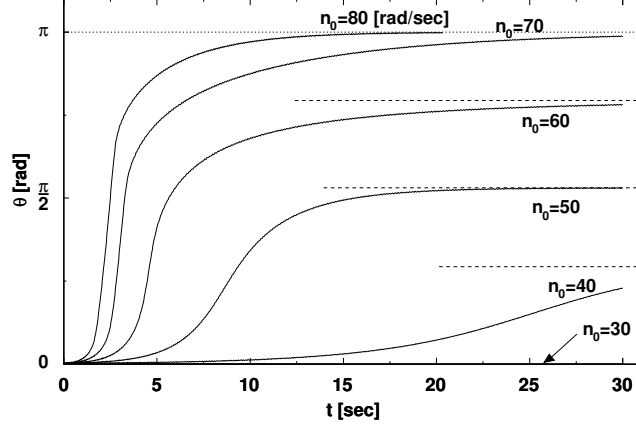


Figure 11: The time evolution of the angle θ for a tippe top of Group II from a spinning position near $\theta = 0$.

5 Summary and Discussion

We have examined an inversion phenomenon of the spinning tippe top, focusing our attention on its relevance to the gyroscopic balance condition (GBC), which was discovered by Moffatt and Shimomura in the study of the spinning motion of a hard-boiled egg. In order to analyze the GBC in detail for the case of the tippe top, we introduce a variable ξ given by (3.1) so that $\xi=0$ corresponds to the GBC, and study the behavior of ξ . Contrary to the case of the spinning egg, the GBC is not satisfied initially for the tippe top. The simulation shows that, starting from a large positive value ξ_0 , the variable ξ for the tippe tops which rise, soon fluctuates around a negative but small value ξ_m such that $|\xi_m/\xi_0| \approx 0$. Thus for these tippe tops, the GBC, though it is not fulfilled initially, will soon be satisfied approximately. Once ξ fluctuates around the value ξ_m , these tops become unstable and start to turn over. On the other hand, in the case of the tippe tops which do not turn over, ξ remains positive around ξ_0 or changes from positive ξ_0 to negative values and then back to positive values close to ξ_0 again.

Under the GBC the governing equations for the tippe top are much simplified and, together with the geometry of the tippe top, we obtain a first-order ODE for θ

in the following form [10] (see (3.5) or (3.7)) :

$$\frac{d\theta}{dt} = b(\theta) . \quad (5.1)$$

It is noted that this equation has a remarkable resemblance to the renormalization group (RG) equation for the effective coupling constant g ,

$$\frac{dg}{dt} = \beta(g) , \quad (5.2)$$

which appears in quantum field theories for critical phenomena [16, 17] and high energy physics [18]. Here in (5.2), t is expressed as $t = \ln\lambda$ with a dimensionless scale parameter λ . Provided that $\beta(g)$ has a zero at $g = g_c$, we find that, if $\beta'(g_c) < 0$, then $g(t) \rightarrow g_c$ as $t \rightarrow \infty$ ($\lambda \rightarrow \infty$), and while if $\beta'(g_c) > 0$, $g(t) \rightarrow g_c$ as $t \rightarrow -\infty$ ($\lambda \rightarrow 0$). The limiting value g_c of $g(t)$ is known as the ultraviolet (infrared) fixed point in the former (latter) case. Similarity between the two equations, (5.1) and (5.2), and the notion of the RG equation brought us to a consequence that tippe tops are classified into three groups, depending on the values of $\frac{A}{C}$ and $\frac{a}{R}$. A resemblance of Eq.(4.2) to the RG equation also gave us a hint that Eq.(4.2) might serve as a criterion for stability of the steady state in Sec. 4.

The criterion (4.2) is a first-order ODE for the (perturbed) inclination angle $\delta\theta$, and the results derived from this criterion coincide with those by ES and BMR which are obtained by mathematically rigorous methods. The key ingredients in the process of arriving at this first-order ODE are the order estimation in μ near the steady states and an intuitive analysis of the equations of motion. The criterion (4.2) can also be applied to the stability analysis of other spinning objects. In fact we have applied (4.2) to the spinning motion of spheroids (prolate and oblate) which was recently examined in detail by MSB [12], and we have obtained consistent results with theirs.

Finally we have assumed, in the present work, a modified version of Coulomb law (2.14) for the sliding friction, since Coulomb friction (2.13) is non-analytic and undefined at $\mathbf{v}_P = 0$. On the other hand, Cohen used Coulomb friction in his pioneering work on the tippe top [4], and analyzed its spinning motion numerically for the first time. He reported the result of a sample simulation in Fig.5 of his

paper [4]. The Coulomb friction is realistic provided that $|\mathbf{v}_P|$ is away from zero, but its application to the spinning motion of the tippe top is very delicate. Near steady states (i.e., near $\theta=0$ or π or θ_s), \mathbf{v}_P almost vanishes (see, for example, Fig.5 (a) and (b)). And there the X - and Y -components of $\mathbf{v}_P/|\mathbf{v}_P|$ are changing signs rapidly and moreover non-analytically, and so are the components of friction, F_X and F_Y . Coulomb friction may not be adequate to be applied to such a situation. In fact, Kane and Levinson [14] argued against the work of Cohen, because it did not include adequate provisions for transitions from sliding to rolling and vice versa. They reanalyzed the simulation of Cohen, assuming Coulomb law for sliding friction, but also providing an algorithm that rolling begins when $|\mathbf{v}_P| < \epsilon$ (with $\epsilon \ll 1\text{m/sec}$) is satisfied, together with another algorithm for the transition from rolling to sliding. They found that a transition from sliding to rolling occurs soon after the motion has begun and that values of θ remain below 0.077 rad thereafter. Or [5] adopted a hybrid friction law adding viscous friction, which is linearly related to \mathbf{v}_P , to Coulomb friction. Other frictional forces such as the one which is due to pure rotation about the normal at the point of contact might have some effect. After all it is safe to say that we have understood general features of the tippe top inversion. But it would be not until we have had thorough knowledge of frictional force that we completely understood the inversion phenomena of the tippe top. *And yet, it flips over.*

Acknowledgments

We thank Tsuneo Uematsu for valuable information on the spinning egg and the tippe top. We also thank Yutaka Shimomura for introducing us to the paper [12] and for helpful discussions.

Appendix

A Equations of motion for the tippe top

We enumerate the equations of motion which are used to analyze the spinning motion of the tippe top:

$$A\dot{\Omega} \sin \theta = (Cn - 2A\Omega \cos \theta)\dot{\theta} + (a - R \cos \theta)F_Y , \quad (\text{A.1})$$

$$A\ddot{\theta} = -\Omega(Cn - A\Omega \cos \theta) \sin \theta - a \sin \theta N - h(\theta)F_X , \quad (\text{A.2})$$

$$C\dot{n} = R \sin \theta F_Y . \quad (\text{A.3})$$

$$M\dot{u}_{OX} = M\Omega u_{OY} + F_X , \quad (\text{A.4})$$

$$M\dot{u}_{OY} = -M\Omega u_{OX} + F_Y , \quad (\text{A.5})$$

$$M\dot{u}_{OZ} = N - Mg . \quad (\text{A.6})$$

$$\mathbf{F} = -\mu N \frac{\mathbf{v}_P}{|\mathbf{v}_P(\Lambda)|} , \quad \text{with } |\mathbf{v}_P(\Lambda)| = \sqrt{v_{PX}^2 + v_{PY}^2 + \Lambda^2} \quad (\text{A.7})$$

$$v_{PX} = u_{OX} - h(\theta)\dot{\theta} , \quad (\text{A.8})$$

$$v_{PY} = u_{OY} + \{R(n - \Omega \cos \theta) + a\Omega\} \sin \theta , \quad (\text{A.9})$$

$$h(\theta) = R - a \cos \theta \quad (\text{A.10})$$

$$u_{OZ} = a \sin \theta \dot{\theta} \quad (\text{A.11})$$

B Stability of the intermediate state

There exists an intermediate steady state for the tippe top of Group II with property $r_c < \frac{A}{C} < 1 + \frac{a}{R}$, when an initial spin $n(\theta=0)$ satisfies $n_1 < n(\theta=0) < n_4$. There is also an intermediate steady state for the tippe top of Group III if $n(\theta=0) > n_1$. In this appendix we show that these steady states are stable.

Near the steady states the primary balance condition (4.10) holds at leading order in μ . Differentiating both sides of (4.10) with respect to t , we obtain

$$(Cn - 2A\Omega \cos \theta)\dot{\Omega} + C\Omega\dot{n} + A\Omega^2 \sin \theta \dot{\theta} = 0 . \quad (\text{B.1})$$

Using (2.6a) and (2.6c), and eliminating $\dot{\Omega}$ and \dot{n} , we find

$$\dot{\theta} = \frac{-F_Y \left\{ (a - R \cos \theta)(Cn - 2A\Omega \cos \theta) + A\Omega R \sin^2 \theta \right\}}{(Cn - 2A\Omega \cos \theta)^2 + (A\Omega \sin \theta)^2} . \quad (\text{B.2})$$

Let $(n_s, \Omega_s, \theta_s)$ represent an intermediate steady state so that n_s , Ω_s and θ_s are related by (4.7a) and (4.7b), and suppose this state to be perturbed to

$$n = n_s + \delta n , \quad \Omega = \Omega_s + \delta \Omega , \quad \theta = \theta_s + \delta \theta . \quad (\text{B.3})$$

Since $\dot{\theta}_s = 0$ and $F_Y|_s = 0$, the perturbed state satisfies

$$\delta \dot{\theta} = -\delta F_Y \frac{RT_s}{C\Omega_s \left\{ S_s^2 + \left(\frac{A}{C} \sin \theta_s \right)^2 \right\}} , \quad (\text{B.4})$$

where

$$S_s = -\frac{Cn_s - 2A\Omega_s \cos \theta_s}{C\Omega_s} = 2\frac{A}{C} \cos \theta_s - \left(\cos \theta_s - \frac{a}{R} \right) , \quad (\text{B.5})$$

$$T_s = S_s \left(\cos \theta_s - \frac{a}{R} \right) + \frac{A}{C} \sin^2 \theta_s . \quad (\text{B.6})$$

At leading order in μ , we have $v_{PY} = v_{\text{rot}PY}$ (recall $u_{OY} \sim \mathcal{O}(\mu^2)$), and thus we obtain from (2.8b),

$$\begin{aligned} \delta F_Y &= -\frac{\mu Mg}{\Lambda} \delta v_{\text{rot}PY} \\ &= -\frac{\mu Mg}{\Lambda} R \sin \theta_s \left\{ \delta n + \left(\frac{a}{R} - \cos \theta_s \right) \delta \Omega + \Omega_s \sin \theta_s \delta \theta \right\} \end{aligned} \quad (\text{B.7})$$

Now we expect that the perturbed state still satisfies the primary balance condition (4.10), since $A\ddot{\theta}$ and F_X are $\mathcal{O}(\mu^2)$. Then a variation around the steady state gives

$$\delta n - S_s \delta \Omega + \frac{A}{C} \Omega_s \sin \theta_s \delta \theta = 0 . \quad (\text{B.8})$$

where S_s is given by (B.5). Also taking a variation of Jellett' constant (4.27) around the steady state (and then, of course, we have $\delta J = 0$), we obtain

$$(\cos \theta_s - \frac{a}{R})\delta n + \frac{A}{C} \sin^2 \theta_s \delta \Omega + S_s \Omega_s \sin \theta_s \delta \theta = 0 . \quad (\text{B.9})$$

From (B.8) and (B.9), δn and $\delta \Omega$ are expressed in terms of $\delta \theta$ as

$$\delta n = -\frac{1}{T_s} \left\{ S_s^2 + \left(\frac{A}{C} \sin \theta_s \right)^2 \right\} \Omega_s \sin \theta_s \delta \theta , \quad (\text{B.10a})$$

$$\delta \Omega = -\frac{1}{T_s} \left\{ S_s - \frac{A}{C} (\cos \theta_s - \frac{a}{R}) \right\} \Omega_s \sin \theta_s \delta \theta . \quad (\text{B.10b})$$

Inserting these expressions into (B.7), and then we obtain from (B.4)

$$\delta \dot{\theta} = -\frac{\mu M g}{\Lambda} \frac{R^2 \sin^2 \theta_s}{C \left\{ S_s^2 + \left(\frac{A}{C} \sin \theta_s \right)^2 \right\}} D(x_s) \delta \theta , \quad (\text{B.11})$$

where

$$D(x_s) = 4 \left[f_1(x_s) \right]^2 + \left(\frac{A}{C} - 1 \right) \sqrt{f_2(x_s)} , \quad (\text{B.12})$$

and $x_s = \cos \theta_s$, and Eqs.(4.31a) and (4.31b) have been used.

If $1 < \frac{A}{C}$, then $D(x_s) > 0$. Also when $r_c < \frac{A}{C} < 1$, $D(x_s)$ is still positive, which is explained as follows: The expression of (4.33a) shows that the function $D(x)$ is related to $F'(x)$ as

$$F'(x) = -\frac{\sqrt{f_2(x)}}{[f_1(x)]^2} D(x) . \quad (\text{B.13})$$

When $r_c < \frac{A}{C} < 1$, an intermediate steady state at $x = x_s$ exists provided $F(-1) > F(1)$ and $F(-1) > \kappa > F(1)$. At that point $F'(x_s)$ is negative, and thus $D(x_s)$ is positive.

C Equivalence between the criterion of ES [7] and Eq.(4.2)

Ebenfeld and Scheck [7] analyzed the stability of the spinning tippe top using the total energy as a Liapunov function and gave the stability criteria for the steady states. We take a different approach to this stability problem. First the system is perturbed around the steady state. Then, using the equations of motion and under the linear approximation, we obtain a first-order ODE for $\delta\theta$ of the form given in (4.2). We make use of this equation and give a different stability criterion. In this appendix we show that both approaches are equivalent and thus they lead to the same conclusions on the stability conditions of the steady states.

ES wrote the total energy of the spinning top as the sum of two terms (ES-(33))⁵

$$E = E^{(1)}(\eta_3, L_{\parallel}) + E^{(2)}(\hat{\boldsymbol{\eta}}, \mathbf{L}_{\perp}, \dot{\mathbf{s}}_{1,2}) , \quad (\text{C.1})$$

the second of which contains all the terms that will vanish at the steady states, while the first depends on $\eta_3 \equiv \cos \theta$ and Jellett's constant J . In terms of the parameters used in this paper, $E^{(1)}$ and $E^{(2)}$ are expressed as follows:

$$E^{(1)} = \frac{J^2}{2AR^2G(\eta_3)} + MgR(1 - \frac{a}{R}\eta_3) , \quad (\text{C.2})$$

$$E^{(2)} = \frac{1}{2}M(u_{OX}^2 + u_{OY}^2 + u_{OZ}^2) + \frac{1}{2}A\dot{\theta}^2 + \frac{(1 - \eta_3^2)G(\eta_3)}{2C(1 - \frac{a}{R}\eta_3)^2} \left\{ \xi + \frac{J \left[\eta_3 - \frac{C}{A}(\eta_3 - \frac{a}{R}) \right]}{RG(\eta_3)} \right\}^2 , \quad (\text{C.3})$$

with

$$G(\eta_3) = 1 - \eta_3^2 + \frac{C}{A}(\eta_3 - \frac{a}{R})^2 , \quad \eta_3 = \cos \theta \quad (\text{C.4})$$

Note that ES set $R=1$. The condition $dE^{(1)}(\theta)/d\theta=0$ together with $u_{OX}=u_{OY}=u_{OZ}=0$ leads to the three solutions of the steady states: (i) vertical spin state at $\theta=0$ (4.5), (ii) vertical spin state at $\theta=\pi$ (4.6), and (iii) intermediate states (4.28), or

⁵From now on, we write the equation (**) of Ref.[7] as ES-(*). The Jellett constant λ defined by ES is related to our J as $\lambda = J/R$.

equivalently, (4.7a-4.7b). It is recalled that we have obtained these solutions starting from equations of motion. At these steady states $E^{(2)}$ vanishes. For intermediate steady states, the factor $\{\xi + J[\eta_3 - \frac{C}{A}(\eta_3 - \frac{a}{R})]/RG(\eta_3)\}$ in (C.3) reduces to zero, due to (4.7a-4.7b) and Jellett's constant given in (4.27).

Now we show that the criterion, Eq.(4.2), for the stability of the steady states is equivalent to the one derived by ES [7]. For the stability analysis of the steady states, the order estimation in μ near the steady states is important, which has been pointed out by MSB in their work on the linear stability analysis of the spinning motion of spheroids [12]. As explained at the beginning of Sec. 4.2, near the steady states we have $\frac{d}{dt} \sim \mathcal{O}(\mu)$, $v_{PX} \sim \mathcal{O}(\mu)$, $v_{PY} \sim v_{\text{rot}PY} \sim \mathcal{O}(1)$, and $u_{OY} \sim \mathcal{O}(\mu^2)$. Since $E^{(2)}$ is already $\mathcal{O}(\mu)$ (recall that it vanishes at the steady states), we have $\frac{dE^{(2)}}{dt} \sim \mathcal{O}(\mu^2)$, while $\frac{dE^{(1)}}{dt} \sim \mathcal{O}(\mu)$. Thus near the steady states, the energy equation (4.3) is written at leading order in μ as

$$\frac{dE^{(1)}}{dt} = \frac{dE^{(1)}}{d\theta} \dot{\theta} = -\mu M g \frac{v_{\text{rot}PY}^2}{|\mathbf{v}_P(\Lambda)|} . \quad (\text{C.5})$$

Suppose the steady states to be perturbed to $n = n_s + \delta n$, $\Omega = \Omega_s + \delta\Omega$, $\theta = \theta_s + \delta\theta$. Since $\dot{\theta}_s = 0$, we have $\dot{\theta} = \delta\dot{\theta}$, and $\frac{dE^{(1)}}{d\theta}$ is expanded as

$$\frac{dE^{(1)}}{d\theta} = \left. \frac{d^2 E^{(1)}}{d\theta^2} \right|_{\theta=\theta_s} \delta\theta + \mathcal{O}\left((\delta\theta)^2\right) , \quad (\text{C.6})$$

where we have used the fact $\left. \frac{dE^{(1)}}{d\theta} \right|_{\theta=\theta_s} = 0$.

Meanwhile $v_{\text{rot}PY}$ is shown to be expressed as

$$v_{\text{rot}PY} = V(n_s, \Omega_s, \theta_s) \delta\theta . \quad (\text{C.7})$$

Actually we have already obtained the expressions (4.13) and (4.22) for $v_{\text{rot}PY}$ ($\approx v_{PY}$) near the steady states at $\theta=0$ and $\theta=\pi$, respectively. Also near the intermediate steady states, δn and $\delta\Omega$ are expressed in terms of $\delta\theta$ as (B.10a) and (B.10b), respectively, and thus we obtain (C.7). Now using Eqs.(C.5)-(C.7) we find

$$\delta\dot{\theta} = -\mu M g \frac{V(n_s, \Omega_s, \theta_s)^2}{|\mathbf{v}_P(\Lambda)|} \frac{1}{\left. \frac{d^2 E^{(1)}}{d\theta^2} \right|_{\theta=\theta_s}} \delta\theta , \quad (\text{C.8})$$

which means that we can identify H in (4.2) as

$$H\left(n_s, \Omega_s, \theta_s, \frac{A}{C}, \frac{a}{R}\right) = \frac{\text{a negative constant}}{\frac{d^2 E^{(1)}}{d\theta^2}\big|_{\theta=\theta_s}}. \quad (\text{C.9})$$

Hence we conclude that the following assertions are equivalent: *a steady state is stable (unstable) $\iff H$ is negative (positive) $\iff \frac{d^2 E^{(1)}}{d\theta^2}\big|_{\theta=\theta_s}$ is positive (negative).*

In fact, ES showed that if the quantity (ES-(39)) with the upper sign is positive, then $\frac{d^2 E^{(1)}}{d\theta^2}\big|_{\theta=\theta_s}$ is positive at $\theta_s=0$ and the non-inverted rotating motion is Liapunov stable. On the other hand, starting from the equations of motion we derived H and obtained the condition (4.16) for the stability of the rotating motion at $\theta_s=0$. It is easily seen that the statement that the quantity (ES-(39)) with the upper sign is positive is equivalent to the inequality given in (4.16), once we know that Jellett's constant at $\theta_s=0$ is given by $J = Cn(\theta_s=0)(R-a)$. Similarly, if the quantity (ES-(39)) with the lower sign is positive, then $\frac{d^2 E^{(1)}}{d\theta^2}\big|_{\theta=\theta_s}$ is positive at $\theta_s=\pi$ and the completely inverted rotating motion is Liapunov stable. The condition that the quantity (ES-(39)) with the lower sign is positive is equivalent to the inequality given in (4.24). Note, this time, $J = Cn(\theta_s=\pi)(-R-a)$.

As for the intermediate steady state ($-1 < \cos \theta_s < 1$), ES stated that if the steady state exists and the quantity (ES-(40)) is negative, then $\frac{d^2 E^{(1)}}{d\theta^2}\big|_{\theta=\theta_s}$ is positive and the state is Liapunov stable. In Sec.4.2.3 we have shown that the stability of the intermediate steady state is determined by the sign of $D(x_s)$ given in (4.40). Now it is interesting to note that $D(x_s)$ is related to (ES-(40)) as follows:

$$D(x_s) = - \frac{A^2 + 3[(A-C)x_s + C\frac{a}{R}]^2}{AC^2} \times (\text{ES.}(40)) . \quad (\text{C.10})$$

Hence the condition that the quantity (ES-(40)) is negative is equivalent to $D(x_s) > 0$. We have seen in Sec.4.2.3 that there exists an intermediate steady state for the tippe top of Group II and also of Group III. (We have not considered a possible intermediate steady state for Group I, since such a state, even if it exists, cannot be reached from the initial spinning position near $\theta = 0$.) For these steady states, we have shown, in Appendix B, that $D(x_s)$ is positive and, therefore, the states are stable.

D Modified Maxwell-Bloch equations and stability criteria [9]

Recently Bou-Rabee, Marsden and Romero [BMR] treated tippe top inversion as a dissipation-induced instability. They showed that the modified Maxwell-Bloch (mMB) equations are a normal form for tippe top inversion and, using the mMB equations and an energy-momentum argument, they gave criteria for the stability on the non-inverted and inverted states of the tippe top [9]. Although we have not explored the connections between the mMB equations and the first-order ODE (4.2) for $\delta\theta$, we show in Appendix D that our results on the stability of the vertical spin states are consistent with the criteria provided by BMR. Actually, rewritten in terms of dimensional parameters and classification criteria used in this paper, the expressions of those criteria become more transparent and they lead to the same stability conditions as ours for the vertical spinning states. Besides, although BMR did not mention, the classification of tippe tops into three groups, Group I, II, and III, according to the behaviors of spinning motion, is possible from the close examination of those criteria.

BMR used the moments of inertia defined as the ones about the principal axes *attached to the center of sphere instead of the center of mass*. The correspondence between the parameters used by BMR and ones in this paper are as follows:

$$\begin{aligned} |e^*| &= \frac{a}{R}, & \frac{1 - \mu e^{*2}}{\sigma} &= \frac{A}{C}, \\ \gamma_Q \Omega_{\text{BMR}} &= -\frac{J}{RC}, & \frac{\mu |e^*| Fr^{-1}}{\sigma} \Omega_{\text{BMR}}^2 &= \frac{Mga}{C}, \end{aligned} \quad (\text{D.1})$$

where Ω_{BMR} is the spin rate of the initially standing equilibrium solution (we added a subscript BMR to distinguish from our Ω), and the dimensionless BMR's ‘‘Jellett’’ constant, γ_Q , is restricted to have a certain value, i.e., $\gamma_Q = -(1 + e^*)$. Also BMR expressed the vector from the center of sphere to the center of mass \overrightarrow{SO} (in the BMR notation \overrightarrow{OC}) as $\overrightarrow{SO} = Re^* \mathbf{k}$, where \mathbf{k} is a unit vector along the symmetry axis. Using the tippe top modified Maxwell-Bloch equations, BMR obtained the stability criteria for the non-inverted state which are given by the three inequalities

in (BMR-(5.3))⁶.

They took $\mathbf{k} = \mathbf{e}_Z$ (upward) in (BMR-(5.3)). Since the non-inverted state has the center of mass below the center of sphere, we have $e^* = -|e^*| = -\frac{a}{R}$, and thus $\Omega_{\text{BMR}} = n(\theta = 0)$. The first inequality of (BMR-(5.3)) is rewritten as $\frac{A}{C} > 0$, which is always satisfied. Apart from some irrelevant positive constants, the second and third inequalities are expressed, respectively, as

$$\frac{Mga}{[n(\theta = 0)]^2 C} \left(1 - \frac{a}{R}\right) \frac{A}{C} + \left(1 - \frac{a}{R}\right)^5 \frac{\nu^2}{\sigma^2} - \frac{A}{C} + \left(1 - \frac{a}{R}\right) > 0, \quad (\text{D.2})$$

$$-\left\{ \frac{A}{C} - \left(1 - \frac{a}{R}\right) - \frac{Mga}{[n(\theta = 0)]^2 C} \left(1 - \frac{a}{R}\right)^2 \right\} > 0. \quad (\text{D.3})$$

From these inequalities, we find:

- (ai) In the case $\frac{A}{C} < (1 - \frac{a}{R})$, i.e., for the tippe top of Group I, the above inequalities are always satisfied. In other words, the non-inverted states ($\theta = 0$) of Group I are always stable.
- (aia) In the case $\frac{A}{C} > (1 - \frac{a}{R})$, i.e., for the tippe tops of Group II or III, the inequality (D.3) is satisfied if

$$[n(\theta = 0)]^2 < \frac{Mga}{C \left\{ \frac{A}{C} - (1 - \frac{a}{R}) \right\}} \left(1 - \frac{a}{R}\right)^2, \quad (\text{D.4})$$

which is the same requirement given in (4.17) for the stability of the tippe top of Group II or III. Note that the inequality (D.2) is automatically satisfied when both $\frac{A}{C} > (1 - \frac{a}{R})$ and inequality (D.3) hold.

Thus, the BMR criteria (BMR-(5.3)) lead to the same result as ours on the stability of the vertical spin state at $\theta = 0$.

The inequalities (BMR-(5.3)), which were derived as the stability criteria for the non-inverted state, can also be used for the stability criteria for the inverted state, but with some replacements. Since $\mathbf{k} = \mathbf{e}_Z$ (upward), the inverted state has the center of mass above the center of sphere. Thus we have $e^* = \frac{a}{R}$ and $\Omega_{\text{BMR}} = -n(\theta = \pi)$.

⁶From now on, we write the equation (**) of Ref.[9] as BMR-(**).

Changing variables in inequalities (D.2) and (D.3) as $a \rightarrow -a$, $\frac{a}{R} \rightarrow -\frac{a}{R}$, and $[n(\theta=0)]^2 \rightarrow [n(\theta=\pi)]^2$, we obtain

$$-\frac{Mga}{[n(\theta=\pi)]^2 C} \left(1 + \frac{a}{R}\right) \frac{A}{C} + \left(1 + \frac{a}{R}\right)^5 \frac{\nu^2}{\sigma^2} - \frac{A}{C} + \left(1 + \frac{a}{R}\right) > 0, \quad (\text{D.5})$$

$$-\left\{ \frac{A}{C} - \left(1 + \frac{a}{R}\right) + \frac{Mga}{[n(\theta=\pi)]^2 C} \left(1 + \frac{a}{R}\right)^2 \right\} > 0, \quad (\text{D.6})$$

for the stability for the inverted state. From the above two inequalities, we see:

- (bi) In the case $\frac{A}{C} > (1 + \frac{a}{R})$, i.e., for the tippe top of Group III, the inequality (D.6) is never satisfied. Therefore, the inverted states ($\theta=\pi$) of Group III are always unstable.
- (bii) In the case $\frac{A}{C} < (1 + \frac{a}{R})$, i.e., for the tippe top of Group I or II, the inequality (D.6) is satisfied if

$$[n(\theta=\pi)]^2 > \frac{Mga}{C\{(1 + \frac{a}{R}) - \frac{A}{C}\}} \left(1 + \frac{a}{R}\right)^2, \quad (\text{D.7})$$

which is the same requirement given in (4.25) for the stability of the tippe top of Group I or II at $\theta=\pi$. The inequality (D.5) is automatically satisfied when both $\frac{A}{C} < (1 + \frac{a}{R})$ and inequality (D.6) hold.

Thus, the BMR criteria (BMR-(5.3)) also lead to the same result as ours on the stability of the vertical spin state at $\theta=\pi$.

Actually, BMR derived also the stability criteria for the inverted state, taking $\mathbf{k} = -\mathbf{e}_Z$, which are given by the three inequalities in (BMR-(5.4))⁷. Of course, we can use them to obtain the stability conditions for the inverted state. Taking now $\Omega_{\text{BMR}} = -\frac{1-e^*}{1+e^*}n(\theta=\pi)$ and $e^* = -\frac{a}{R}$ in the second and third inequality in (BMR-(5.4)), we reach the same conclusions, (bi) and (bii).

BMR discussed in Ref. [9] about the heteroclinic connection between the non-inverted and inverted states of the tippe top. They used an energy-momentum argument to determine the asymptotic states of the tippe top and obtained the

⁷The second inequality should read as $\sigma(1+e^*)^2[\sigma(1-e^*) - (1-\mu e^{*2})] + \nu^2(1-e^*)^7 + (1-e^*)^3 \mu e^* F r^{-1}(1-\mu e^{*2}) > 0$. The error is traced back to the missing factor of $(\gamma_z^0 n^0)$ in the expression of F in BMR-(4.2).

explicit criteria for the existence of a heteroclinic connection, which are given in Theorem 6.2 and the appendix of Ref. [9]. In terms of the classification criteria and conditions obtained in this paper, the statement in BMR on the existence of a heteroclinic connection can be restated as follows: (i) A tippe top must belong to Group II in order to have a heteroclinic connection. (ii) Further more, the initial spin $n(\theta=0)$ should be larger than n_1 (Eq.(4.18)) and n_4 (Eq.(4.42)) so that a tippe top becomes unstable at $\theta=0$ and reaches the inverted position. The requirements $n(\theta=0) > n_1$ and $n(\theta=0) > n_4$, respectively, correspond to the criteria $r_0 > 0$ and $r_4 > 0$ in Theorem 6.2 in BMR.

References

- [1] A. Garcia and M. Hubbard, “Spin reversal of the rattleback: theory and experiment,” *Proc. R. Soc. Lond.* **A418**, 165-197 (1988), and references therein.
- [2] C. M. Braams, “On the influence of friction on the motion of a top,” *Physica* **18**, 503-514 (1952).
- [3] N. M. Hugenholtz, “On Tops Rising by Friction,” *Physica* **18**, 515-527 (1952).
- [4] R. J. Cohen, “The Tippe Top Revisited,” *Am. J. Phys.* **45**, 12-17 (1977).
- [5] A. C. Or, “The Dynamics of a Tippe Top,” *SIAM J. Appl. Math.* **54**, 597-609 (1994).
- [6] H. Leutwyler, “Why Some Tops Tip,” *Eur. J. Phys.* **15**, 59-61 (1994).
- [7] S. Ebenfeld and F. Scheck, “A New Analysis of the Tippe Top: Asymptotic States and Liapunov Stability,” *Annals of Physics*. **243**, 195-217 (1995).
- [8] C. G. Gray and B. G. Nickel, “Constants of the motion for nonslipping tippe tops and other tops with round pegs,” *Am. J. Phys.* **68**, 821-828 (2000), and references therein.
- [9] N. M. Bou-Rabee, J. E. Marsden and L. A. Romero, “Tippe top inversion as a dissipation induced instability,” *SIAM J. Applied Dynamical Systems*, **3**, 352-377 (2004).
- [10] H. K. Moffatt and Y. Shimomura, “Spinning eggs—a paradox resolved,” *Nature* **416**, 385-386 (2002).
- [11] K. Sasaki, “Spinning eggs—which end will rise?,” *Am. J. Phys.* **72**, 775-781 (2004).
- [12] H. K. Moffatt, Y. Shimomura and M. Branicki, “Dynamics of an axisymmetric body spinning on a horizontal surface. Part I: Stability and the gyroscopic approximation,” *Proc. Roy. Soc. A* **460**, 3643-3672 (2004).

- [13] J. H. Jellett, *A Treatise on the Theory of Friction* (MacMillan, London, 1872).
- [14] T. R. Kane and D. A. Levinson, “A Realistic Solution of the Symmetric Top Problem,” *J. Appl. Mech.* **45**, 903-909 (1978).
- [15] T. Sakai, “Tippe tops,” *Suuri Kagaku (Mathematical Science)* **211**, 30-36 (1981) (in Japanese).
- [16] K. G. Wilson and J. Kogut, “The Renormalization Group and the ϵ Expansion,” *Physics Reports* **12C**, 75-200 (1974).
- [17] J. Zinn-Justin, *Quantum Field Theory and Critical Phenomena* (Oxford University Press, Oxford, 1996).
- [18] T. Muta, *Foundations of Quantum Chromodynamics* (World Scientific, Singapore, 1987).